PURDUE RESEARCH FOUNDATION
Project Nos. 5250 and 5567

TECHNICAL REPORT FMTR-70-1
December 1970

SHOCK INDUCED BOUNDARY LAYER OVER A SEMI-INFINITE FLAT PLATE

Part I

Flow in the Immediate Vicinity of the Shock Wave

by

Douglas E. Abbott and Michael I. O. Ero

SCHOOL OF MECHANICAL ENGINEERING
FLUID MECHANICS GROUP
PURDUE UNIVERSITY

Technical Report FMTR 70-1

December 1970

NATIONAL AERONAUTICS AND SPACE ADMINISTRATION
Grant No. NGR 15-005-077

COPY NO. 42

SHOCK INDUCED BOUNDARY LAYER OVER A SEMI-INFINITE FLAT PLATE

Part I

Flow in the Immediate Vicinity of the Shock Wave

by

Douglas E. Abbott and Michael I. O. Ero

PURDUE RESEARCH FOUNDATION
Project No. 5250 and 5567

NATIONAL AERONAUTICS AND SPACE ADMINISTRATION
Grant No. NGR 15-005-077

School of Mechanical Engineering
Fluid Mechanics Group
Purdue University

Technical Report FMTR-70-1

December 1970

ABSTRACT

The problem considered in this report is the laminar, two-dimensional boundary layer generated in the immediate vicinity of a plane shock wave moving over a flat plate into a gas initially at rest. Results are obtained for both a perfect gas and a real gas in thermodynamic equilibrium (nitrogen). The analytical method employed in the present study is the method of weighted residuals or MWR. It is shown that the MWR first approximation agrees within six percent with the results for skin friction coefficient given by Mirels and modified by Lam and Crocco for a perfect gas; an MWR second approximation is also computed and shows agreement within one percent or better. Real gas solutions are calculated for an MWR second approximation and compared with the perfect gas results. The primary utility of the present work is its application to the shock induced flow over a semi-infinite flat plate where the leading-edge is taken into account. This extension, assuming boundary-layer approximations, is given in a companion report.

ACKNOWLEDGMENTS

The authors wish to acknowledge Purdue University for providing computer funds during the early phases of this work and NASA-Ames Research Center for their support under Grant 15-005-077. In particular, thanks are given to Mr. M. W. Rubesin and Mr. L. L. Presley of NASA-Ames for their help and constructive criticism at various stages of the work, and to Professors F. P. Incropera and F. J. Marshall and Doctors S. J. Koob and G. S. Deiwert for their valuable discussions. The work on which this report is based has been up-dated from the Ph.D. Thesis of Dr. M. I. O. Ero, completed in March, 1968.

TABLE OF CONTENTS

LIST OF SYMBOLS

C_f - Skin friction coefficient, $\left(\mu \frac{\partial u}{\partial y}\right)_{y=0} \Big/ \rho_e U_e^2$

C_p - Specific heat at constant pressure, Btu/lbm °F

f - Weighting function defined by equations (3.18) and (5.20)

g_c - Gravitational constant, 32.174 ft/sec^2

h - Dimensional static enthalpy, Btu/lbm

J - Joule mechanical equivalent of heat, 778.16 ft-lbf/Btu

K - Thermal conductivity, Btu/ft hr °F

L - Characteristic length

P - Static pressure outside boundary layer; also a dummy variable defined in (3.12)

Pr - Prandtl number $\mu C_p/K$

Q - Dummy variable in equation (3.15)

R - Gas constant for Nitrogen gas, 55.15 ft-lbf/lb-mole °R

Re_L - Reynolds number defined by $\rho_e U_e L/\mu_e$

t - Time

u - Velocity parallel to flat plate

v - Transverse velocity

w - The ratio of velocities across a stationary normal shock

x - Longitudinal independent variable

y - Transverse independent variable

δ - Boundary-layer thickness, equations (5.26c) and (D.11)

δ^* - Displacement thickness, equations (5.26d) and (D.12)

δ^{**} - Momentum thickness, equations (5.26e) and (D.13a)

δ^{***} - Energy dissipation thickness, equations (5.26f) and (D.13b)

η - Nondimensional transverse coordinate, $\sqrt{U_e/\nu_e L}\ y$

μ - Dynamic viscosity

ν - Kinematic viscosity

ϕ - Nondimensional transport variable, $\rho\mu/\rho_e\mu_e$

ρ - Density

ψ - Dummy variable used in (5.19)

ξ - Nondimensional longitudinal variable, x/L

τ - Nondimensional time variable, $U_e t/L$

θ - Inverse of the gradient of the nondimensional velocity given by $(\partial u^*/\partial\eta)^{-1}$

Subscripts and Superscripts

e - Variable evaluated outside the boundary layer

i - Indexing subscript as in h_o, h_1, etc.

L - Characteristic length of flat plate

m - Used with respect to η such that $\eta_m = \sqrt{U_e/2x\nu_w}\int_o^y \rho/\rho_w\, dy$

n - Nodal index

w - Value of a variable evaluated at the wall

* - Denotes variable nondimensionalized with respect to its value at the outer edge of the boundary layer in plate fixed coordinates

** - Variable nondimensionalized with respect to its value at the outer edge of the boundary layer in shock wave fixed coordinates

^ - Dimensional variable in shock wave fixed coordinates

1. INTRODUCTION

The problem to be considered in this report is the viscous flow in the immediate vicinity of a plane shock wave moving over a flat surface into a gas initially at rest. The flow will be assumed to satisfy the laminar boundary-layer equations with zero pressure gradient. While such assumptions are not well satisfied on the walls of shock tubes, they are reasonably good approximations for the shock induced flow on a shock tube splitter plate. Solutions for this problem have been reported by a number of investigators, including Mirels [1], Ackroyd [2,3], and as a part of the analysis of Lam and Crocco [4]. Thus, the results for a perfect gas to be reported here will not be new. Rather, the purpose of the present work is to first, present a new method of analysis for such flows and make comparisons with the earlier work, and second, to develop the basis for the extension of the new method to include the leading edge effects of the splitter plate and thus analyze the complete semi-infinite splitter plate problem (the complete analysis is given in a companion report).

The flow under consideration is shown in Figure 1. Figure 1a represents the unsteady flow as seen by an observer fixed relative to the wall. By assuming that there is no

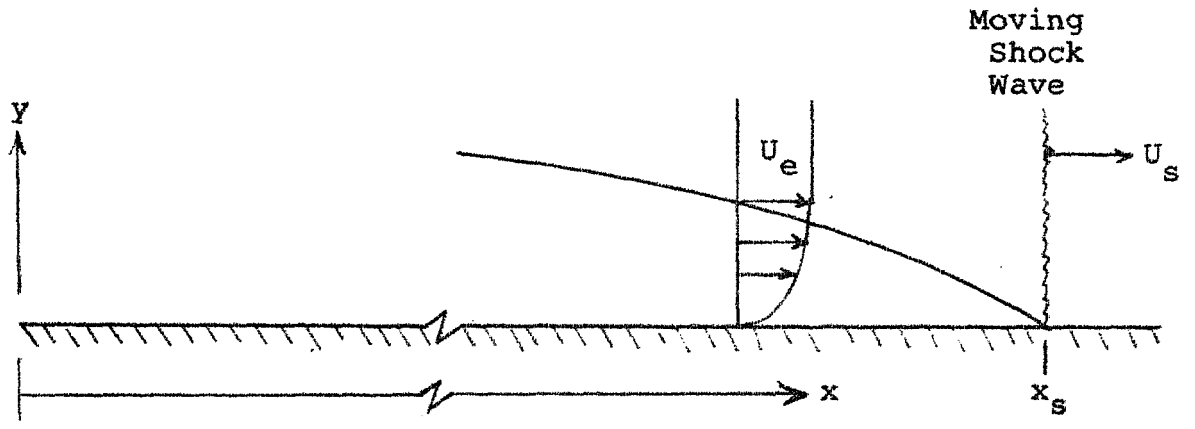

(a) Flow Relative to the Plate.

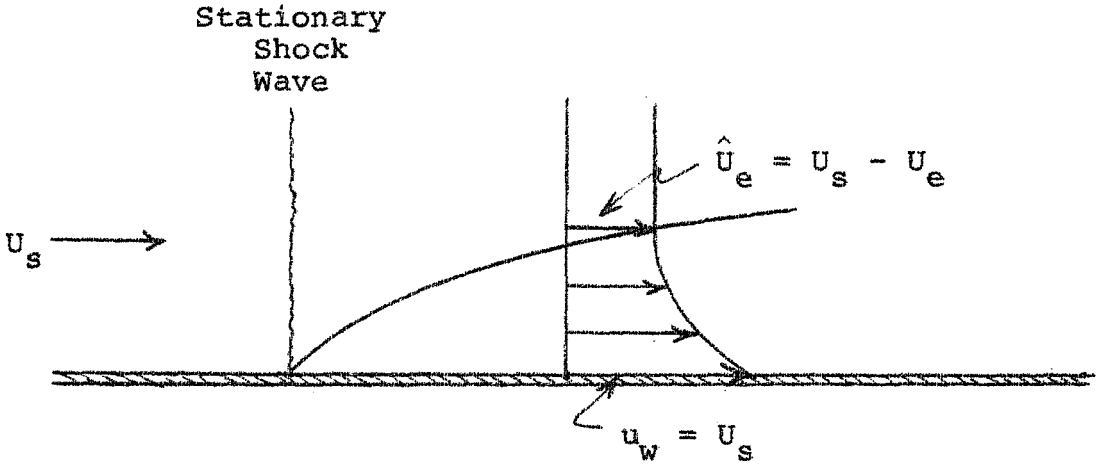

(b) Flow Relative to the Shock Wave.

Figure 1: The Boundary Layer Behind a Moving Shock Wave.

attenuation of the shock wave, the problem may be considered as quasi-steady by considering the flow relative to the shock wave, see Figure 1b. Solutions in either reference frame must, of course, be equivalent, however the quasi-steady approach is simpler to analyze because time does not enter explicitly as an independent variable and the previous work on this problem has taken advantage of this factor. The analysis to be reported here will consider, to some extent, both reference frames. However, the majority of the analysis will be for the unsteady flow case because the ultimate goal of the present analysis will be its extension to include the plate leading edge; a problem for which the flow is truly unsteady both relative to the plate and the shock wave.

The present analysis will consider solutions for both a perfect gas and a real gas in thermodynamic equilibrium. Although the flow to be analyzed is considered to model conditions in a shock tube, the variation of thermodynamic variables such as density and enthalpy are assumed to be monotonic in accordance with the earlier work which will be used as a basis of comparison for the present results. Thus, even though real gas solutions will be developed, a restricted range of shock wave velocities is inherently assumed.

The analytical method employed in the present work is the method of weighted residuals or MWR. It will be shown that an MWR first approximation is in excellent agreement with the results of Mirels [1] who employed an integral technique and

the results of Lam and Crocco [4] who used a numerical finite difference method. Results for an MWR second approximation will also be given for both a perfect and a real gas (nitrogen).

2. MATHEMATICAL FORMULATION

The flow under consideration is a laminar two-dimensional boundary layer generated by a plane shock wave moving over a flat plate and is shown in Figure 1. Relative to the plate, the shock wave is located at a point $x_s(t)$, where $x_s(t) = U_s t$ and U_s is the velocity of the shock, measured with respect to the leading edge of the plate which is assumed far upstream and out of consideration of the present analysis (a companion report will consider the effect of the plate leading edge). Time is also measured relative to the shock wave arrival at the leading edge, but this too is not relevant to the present analysis. The following assumptions are made:

(i) The shock wave is plane, attached to the plate, and does not attenuate with time.

(ii) The conditions outside the boundary layer behind the moving shock wave are adequately related to the conditions ahead of the shock by the Rankine-Hugoniot relation for a normal shock.

(iii) The boundary layer is laminar, at constant pressure, and is adequately described by the classical two-dimensional unsteady boundary-layer equations for a compressible flow.

(iv) The fluid is considered to be either a perfect gas with constant Prandtl number, or a real gas in thermodynamic equilibrium.

Under the above assumptions, the following governing equations are obtained for flow relative to the plate:

Continuity

$$\frac{\partial \rho}{\partial t} + \frac{\partial \rho u}{\partial x} + \frac{\partial \rho v}{\partial y} = 0 \tag{2.1}$$

Momentum

$$\rho \frac{\partial u}{\partial t} + \rho u \frac{\partial u}{\partial x} + \rho v \frac{\partial u}{\partial y} = \frac{\partial}{\partial y}\left(\mu \frac{\partial u}{\partial y} \right) \tag{2.2}$$

$$\frac{\partial P}{\partial y} = 0 \tag{2.3a}$$

$$\frac{\partial P}{\partial x} = 0 \text{ (flat plate case)} \tag{2.3b}$$

Energy

$$\rho \frac{\partial h}{\partial t} + \rho u \frac{\partial h}{\partial x} + \rho v \frac{\partial h}{\partial y} = \frac{\partial}{\partial y}\left(\frac{\mu}{Pr} \frac{\partial h}{\partial y} \right) + \frac{\mu}{g_c J}\left(\frac{\partial u}{\partial y} \right)^2 \tag{2.4}$$

The thermodynamic and transport property relations are assumed in the form:

$$\left.\begin{aligned} \rho &= \rho(h) \\ \mu &= \mu(h) \\ Pr &= Pr(h) \end{aligned}\right\} \tag{2.5}$$

The boundary conditions for velocity and enthalpy distributions are:

$$u(x > x_s, y, t) = 0 \tag{2.6a}$$

$$v(x > x_s, y, t) = 0 \tag{2.6b}$$

$$u(x, 0, t) = 0 \tag{2.6c}$$

$$v(x, 0, t) = 0 \tag{2.6d}$$

$$u(x, y \to \infty, t) \to U_e \tag{2.6e}$$

$$u(x_s, y > 0, t) = U_e \tag{2.6f}$$

$$h(x > x_s, y, t) = h_w \tag{2.6g}$$

$$h(x, 0, t) = h_w \tag{2.6h}$$

$$h(x, y \to \infty, t) \to h_e \tag{2.6i}$$

$$h(x_s, y > 0, t) = h_e \tag{2.6j}$$

where u is the longitudinal velocity parallel to, and v is the transverse velocity perpendicular to, the plate, respectively. It will also be assumed that the wall temperature remains constant during the flow. Thus

$$h_w = \text{constant} \tag{2.6k}$$

This last assumption can be justified by the large thermal capacity of the splitter plate and the short duration of shock tube flows.

It is convenient to normalize the dependent variables in equations (2.1) to (2.6) with respect to their values in the freestream, and to define nondimensional independent variables as follows:

$$u^* = \frac{u}{U_e} \tag{2.7a}$$

$$v^* = v \sqrt{\frac{L}{\nu_e U_e}} \tag{2.7b}$$

$$h^* = \frac{h}{h_e} \tag{2.7c}$$

$$\rho^* = \frac{\rho}{\rho_e} \tag{2.7d}$$

$$\mu^* = \frac{\mu}{\mu_e} \tag{2.7e}$$

$$\phi = \rho^* \mu^* \tag{2.7f}$$

$$\xi = \frac{x}{L} \tag{2.7g}$$

$$\eta = \sqrt{\frac{U_e}{\nu_e L}}\, y \tag{2.7h}$$

$$\tau = \frac{U_e t}{L} \tag{2.7i}$$

where L is an arbitrary reference length. Under the above transformation, the governing equations become:

Continuity

$$\frac{\partial \rho^*}{\partial \tau} + \frac{\partial \rho^* u^*}{\partial \xi} + \frac{\partial \rho^* v^*}{\partial \eta} = 0 \tag{2.8}$$

Momentum

$$\rho^* \frac{\partial u^*}{\partial \tau} + \rho^* u^* \frac{\partial u^*}{\partial \xi} + \rho^* v^* \frac{\partial u^*}{\partial \eta} = \frac{\partial}{\partial \eta}\left(\mu^* \frac{\partial u^*}{\partial \eta}\right) \tag{2.9}$$

Energy

$$\rho^* \frac{\partial h^*}{\partial \tau} + \rho^* u^* \frac{\partial h^*}{\partial \xi} + \rho^* v^* \frac{\partial h^*}{\partial \eta} = \frac{\partial}{\partial \eta}\left(\frac{\mu^*}{Pr} \frac{\partial h^*}{\partial \eta}\right) + \frac{U_e^2}{g_c J h_e} \mu^* \left(\frac{\partial u^*}{\partial \eta}\right)^2 \tag{2.10}$$

Property equations

$$\rho^* = \rho^*(h^*) \tag{2.11a}$$

$$\mu^* = \mu^*(h^*) \tag{2.11b}$$

$$Pr = Pr(h^*) \tag{2.11c}$$

Boundary Conditions

$$u^*(\xi > \xi_s, \eta, \tau) = 0 \tag{2.12a}$$
$$v^*(\xi > \xi_s, \eta, \tau) = 0 \tag{2.12b}$$
$$u^*(\xi, 0, \tau) = 0 \tag{2.12c}$$
$$v^*(\xi, 0, \tau) = 0 \tag{2.12d}$$
$$u^*(\xi, \eta \to \infty, \tau) \to 1 \tag{2.12e}$$
$$u^*(\xi_s, \eta > 0, \tau) = 1 \tag{2.12f}$$
$$h^*(\xi > \xi_s, \eta, \tau) = h_w/h_e \tag{2.12g}$$
$$h^*(\xi, 0, \tau) = h_w/h_e \tag{2.12h}$$
$$h^*(\xi, \eta \to \infty, \tau) \to 1 \tag{2.12i}$$
$$h^*(\xi_s, \eta > 0, \tau) = 1 \tag{2.12j}$$

Equations (2.8), (2.9), and (2.10) are partial differential equations in the three independent variables ξ, η, and τ. It is well known (see, for example, Mirels [1]) that these three equations may be reduced to a system of two coupled ordinary differential equations by following two steps: first, by transforming to shock-fixed coordinates which eliminates τ, and then employing a similarity transformation that combines ξ and η into a single variable. Additionally, there is a transformation first proposed by Stewartson and employed in detail by Lam and Crocco [4] and Hall [5,6,7] which combines the three plate-fixed variables into two similarity variables. While these similarity transformations do have an advantage for analysis of the present problem of flow behind a shock wave, they prove to be of more academic rather than analytical interest in the general case where the leading edge is considered. Thus,

in the present report, the full equations (2.8), (2.9), and (2.10) will be analyzed in the next section by the method of weighted residuals (MWR). It will be shown in a later section that the resulting MWR first approximation leads to an analytical solution which provides considerable insight into the problem in general, as well as setting the stage for the treatment of the more general, and interesting, leading edge problem. It will be shown in the present work however, that higher MWR approximations than the first can best be obtained numerically by reverting to the shock-fixed coordinates, although when the leading edge effect is included in the companion report, this analytical advantage is lost and the present formulation as given above is again employed for all orders of MWR approximation.

3. ANALYSIS BY THE METHOD OF WEIGHTED RESIDUALS

An analysis will now be developed to reduce the governing equations and boundary conditions (2.8) to (2.12) in three independent variables to a system of equations in two independent variables. This reduction will be achieved by employing the method of weighted residuals or MWR, a technique that has been used in the past for a variety of boundary-layer problems (see [8,9,10,11,12,13]). The general theory underlying the MWR has been extensively reviewed and discussed in References 8 and 9 and will not be repeated here, however the analytical details of the method as applied to the present problem will now be carefully outlined.

The various steps of the method may be described as follows. First, equation (2.8) is multiplied by $f_i(u^*)$ and (2.9) by $df_i(u^*)/du^*$ where $f_i(u^*)$, the "weighting function", is a function of u^*, temporarily assumed arbitrary; the resulting two equations are added, yielding

$$\frac{\partial}{\partial \tau}\left(\rho^* f_i(u^*)\right) + \frac{\partial}{\partial \xi}\left(\rho^* u^* f_i(u^*)\right) + \frac{\partial}{\partial \eta}\left(\rho^* v^* f_i(u^*)\right) = f_i'(u^*)\frac{\partial}{\partial \eta}\left(\mu^* \frac{\partial u^*}{\partial \eta}\right) \tag{3.1}$$

Second, equation (2.10) is multiplied by $f_i(u^*)$ and equation (3.1) by h^*; the two resulting equations are added together to yield

$$\frac{\partial}{\partial\tau}\left(\rho^*h^*f_i(u^*)\right) + \frac{\partial}{\partial\xi}\left(\rho^*h^*f_i(u^*)\right) = h^*f_i'(u^*)\frac{\partial}{\partial\eta}\left(\mu^*\frac{\partial u^*}{\partial\eta}\right)$$
$$+ f_i(u^*)\frac{\partial}{\partial\eta}\left(\frac{u^*}{Pr}\frac{\partial h^*}{\partial\eta}\right) + \frac{U_e^2}{g_cJh_e}f_i(u^*)\mu^*\left(\frac{\partial u^*}{\partial\eta}\right)^2 \qquad (3.2)$$

Third, the resulting equations (3.1) and (3.2) are integrated with respect to η from 0 to ∞, and the variable of integration is changed from η to u^* yielding the following integro-differential equations:

$$\frac{\partial}{\partial\tau}\int_0^1 f_i(u^*)\rho^*\theta du^* + \frac{\partial}{\partial\xi}\int_0^1 f_i(u^*)\rho^*\theta u^*du^* =$$
$$-\left(f_i'(u^*)\frac{\phi}{\rho^*\theta}\right)_{u^*=0} - \int_0^1 f_i''\frac{\phi}{\rho^*\theta}\,du^* \qquad (3.3)$$

$$\frac{\partial}{\partial\tau}\int_0^1 f_i(u^*)h^*\rho^*\theta du^* + \frac{\partial}{\partial\xi}\int_0^1 f_i(u^*)h^*\rho^*\theta u^*du^* =$$
$$-\left(f_i(u^*)\frac{\partial h^*}{\partial u^*}\frac{\phi}{Pr}\frac{1}{\rho^*\theta}\right)_{u^*=0} - \left(f_i'(u^*)h^*\frac{\phi}{\rho^*\theta}\right)_{u^*=0}$$
$$-\int_0^1\left(\phi + \frac{\phi}{Pr}\right)\frac{\partial h^*}{\partial u^*}\frac{f_i'(u^*)}{\rho^*\theta}\,du^* - \int_0^1 h^*f_i''(u^*)\frac{\phi}{\rho^*\theta}\,du^*$$
$$+ \frac{U_e^2}{g_cJh_e}\int_0^1\frac{\phi}{\rho^*\theta}f_i(u^*)\,du^* \qquad (3.4)$$

where $$\theta = \left(\frac{\partial u^*}{\partial\eta}\right)^{-1} \qquad (3.5)$$

Recognizing that the function $\theta(\xi,u^*,\tau)$ defined by equation (3.5) is proportional to the inverse of the shear stress, and that θ now replaces u^* in the governing equations as a dependent variable, the appropriate boundary conditions may be written as:

$$\theta(\xi_s,u^*,\tau) = 0 \tag{3.6a}$$

$$h^*(\xi_s,u^*>0,\tau) = 1 \tag{3.6b}$$

In general it is not possible to obtain analytic solutions to equations (3.3) and (3.4). However, by suitably approximating the dependent variables θ and h^* (as well as $\rho^*(h^*)$), selecting appropriate variations of the physical properties ϕ and Pr, and employing the weighting function $f_i(u^*)$ to assure that certain mathematical requirements are satisfied, approximate solutions may be formulated to provide (theoretically) any desired accuracy. The selection of the approximating and weighting functions is not completely arbitrary but must be guided by both physical and mathematical requirements. These requirements will now be examined in some detail.

3.1 Approximating and Weighting Functions

It is not possible a priori to formulate the exact functional expressions for ρ^*, h^* and θ. However these functions may be approximated by suitable expressions which preserve known physical characteristics across the boundary layer. The formulation of these approximating functions will

be discussed in Section 3.1.1. Replacement of the exact expressions for ρ^*, θ, and h^* in equations (3.3) and (3.4) by the corresponding functional approximation completes the reduction to a problem in two independent variables, ξ and τ. The sense in which the integro-differential equations remain exact upon substitution of the approximating function is revealed through the proper interpretation of the weighting function $f_i(u^*)$; the $f_i(u^*)$ must be chosen first with the view that the error developed by replacing exact functional relations by approximate expressions and weighted by the functions $f_i(u^*)$ is zero over the range of the integration. In general, therefore, the role of $f_i(u^*)$, $i = 1, 2,...N$, is to preserve the sense in which the integro-differential equations are exact even when ρ^*, θ, and h^* are replaced by approximating functions. In the analytical sense, it is clear that the $f_i(u^*)$ are orthogonal to the error in the interval $0<u^*<1$. Error equations of the type defined above will, in subsequent sections, be called the residual equations. The derivation of the weighting function is discussed in Section 3.1.2.

The orthogonality requirement above imposes an additional constraint on all the free parameters which go into defining the approximating functions. By using weighting functions $f_i(u^*)$, $i = 1, 2,...N$, it is possible to obtain N simultaneous partial differential equations which determine N free parameters used in the approximating function. Thus in addition to satisfying the known physical characteristic of ρ^*, θ and h^*, it is

possible to use an arbitrary number of free parameters to ensure their accurate determination.

The technique described above is the classical method of weighted residuals. Its similarity to the Kármán-Pohlhausen integral method is clear, where it will be recalled that the approximation function for the velocity profile is obtained from the no slip condition at the wall, and compatibility at the outer edge of the boundary layer.

3.1.1 Approximating Functions

The first prerequisites in the selection of approximating functions are that the proper physical characteristics of the functions must be assured by the assumed mathematical formulation, and that the resulting integrals must be bounded and should be such that they can be either evaluated analytically or to sufficient accuracy by numerical computation.

Advantage may be taken of the occurrence of functional groups in equations (3.3) and (3.4) as a clue in formulating the approximation functions. Because the group $\rho^*\theta$ always appears together, it is convenient to write a single approximation for this product. But before doing this, it is instructive to observe that, physically, $\rho^*\theta$ represents the product of the nondimensional density ratio ρ^* and the inverse of the nondimensional velocity gradient $\theta = (\partial u^*/\partial \eta)^{-1}$. The conditions to be satisfied by the approximating function for the product of ρ^* and θ can be rationalized by considering their individual qualitative behavior.

In Sketch 1a is shown the velocity distribution associated with a zero pressure gradient flow of a fluid over a stationary flat plate. The velocity grows uniformly from zero at the wall to the velocity at the edge of the boundary layer. Thus in general, the velocity distribution satisfies the following conditions

$$u^*(\xi,0,\tau) = 0 \tag{3.7a}$$

$$u^*(\xi,\eta\geq\delta,\tau) = 1 \tag{3.7b}$$

$$\frac{\partial u^*}{\partial \eta}(\xi,\eta\geq\delta,\tau) = 0 \tag{3.7c}$$

where δ is the local boundary-layer thickness. From the trends in Sketch 1a, the qualitative form of the velocity gradient and its inverse in shown in Sketch 1b.

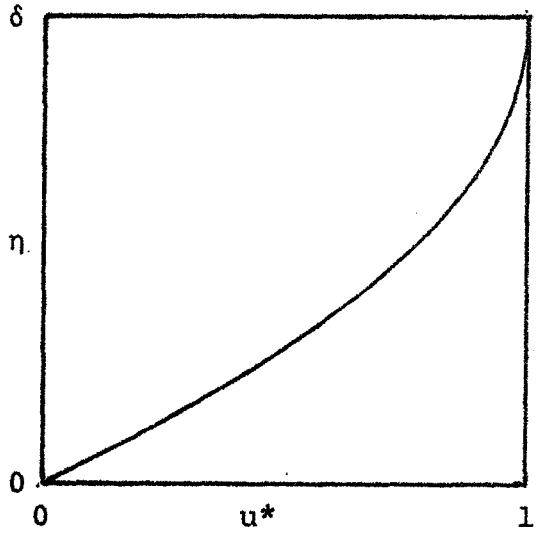

Sketch 1a

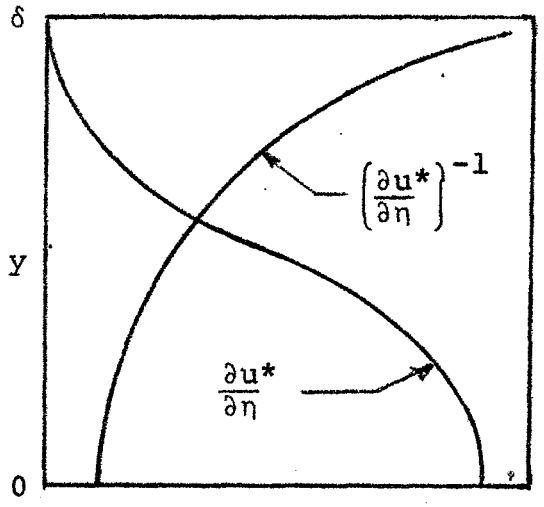

Sketch 1b

The foregoing discussion suggests that the approximating function chosen for the inverse of the velocity gradient must preserve the following characteristics.

$$\theta(\xi,0,\tau) = \text{finite} \tag{3.8a}$$

$$\theta(\xi,1,\tau) = \infty \tag{3.8b}$$

The representation of θ with a polynomial is complicated by the fact that θ tends to infinity as u^* tends to one. Thus, a singularity of θ of at least the first order exists at $u^* = 1$. It is necessary to characterize this singularity by as high an order as possible if compatibility conditions at the edge of the boundary layer are to be enforced. However, it is not particularly helpful to impose compatibility conditions since the outer edge of the boundary layer is usually taken as satisfactorily fixed at a point where the boundary-layer velocity approaches to within 99 percent of the freestream velocity. Therefore assuming θ has a first order singularity at $u^* = 1$, the function may be represented by

$$\theta = \frac{1}{1-u^*} \sum_{i=0}^{N-1} a_i(\xi,\tau) u^{*i} \tag{3.9}$$

where $N = 1, 2, \ldots$ is associated with the order of approximation of the unknown variable.

The nondimensional density ratio ρ^* varies between unity at the outer edge of the boundary layer and a value of ρ_w/ρ_e at the wall. The value of ρ_w/ρ_e in general depends on the

prescribed wall conditions. In shock tube applications, ρ_w/ρ_e may vary from unity for an acoustic wave to a number greater than one for moderate intensity shock waves. Variations of ρ^* within the boundary layer depend on a combination of frictional heating and the wall value. For the present case of moderate intensity shock waves, it will be assumed that an adequate approximation for $\rho^*\theta$ may be written as:

$$\rho^*\theta = \frac{1}{1-u^*} \sum_{i=0}^{N-1} b_i(\xi,\tau)\ u^{*i} \tag{3.10}$$

consistant with equation (3.9).

The variation of the nondimensional density and enthalpy ratios ρ^*, h^*, and the thermodynamic and transport property ratios $\phi = \rho\mu/\rho_e\mu_e$ and $g = (\rho\mu/Pr)/(\rho_e\mu_e/Pr_e)$ can be represented by a dummy variable $P(\xi,u^*,\tau)$ which has the following characteristics:

$$P(\xi,0,\tau) = P_w \tag{3.11a}$$

$$P(\xi,1,\tau) = 1 \tag{3.11b}$$

where

$$P \equiv \left\{ \begin{array}{l} \rho/\rho_e \\ \rho\mu/\rho_e\mu_e \\ h/h_e \\ (\rho\mu/Pr)/(\rho_e\mu_e/Pr_e) \end{array} \right\} \tag{3.12}$$

A suitable approximation for P is assumed to be

$$P(\xi,u^*,\tau) = \sum_{i=0}^{N-1} c_i(\xi,\tau)\ u^{*i} \tag{3.13}$$

It is convenient to formulate a separate approximating function for the inverse of $\rho^*\theta$ whenever this occurs on the right hand side of the integro-differential equations (3.3) and (3.4). However, it is helpful to note that in the integro-differential equation, the inverse of $\rho^*\theta$ occurs only as $\phi/\rho^*\theta$ or $(\phi/Pr)/\rho^*\theta$. In general therefore, whenever the inverse of $\rho^*\theta$ occurs as the group $Q/\rho^*\theta$, the following approximation is used

$$\frac{Q}{\rho^*\theta} = (1-u^*) \sum_{i=0}^{N} d_i(\xi,\tau)\ u^{*i} \qquad (3.14)$$

where the dummy variable, Q, is given by

$$Q \equiv \left\{ \begin{array}{l} \phi \\ \phi/Pr \\ \phi + \phi/Pr \end{array} \right\} \qquad (3.15)$$

This form has been used by Pavlovskii [13] in the study of steady compressible flow over a blunt body with spherical leading edge and cylindrical trailing edge.

Specification of the various approximating functions is now achieved. It remains to complete the analysis by selecting the weighting functions.

3.1.2 Weighting Functions

It has been noted that the weighting functions $f_i(u^*)$, $i = 1,2,...N$, preserve the sense in which equations (3.3) and (3.4) are exact mathematical expressions. In Section 3.1, it was deduced that the $f_i(u^*)$ are orthogonal to the residual equations in the interval $0<u^*<1$. In addition to this orthogonality condition, it is necessary in equations (3.3) and

(3.4), that the $f_i(u^*)$ be linearly independent; that is, it should be impossible to find a real set of nonzero λ_i such that

$$\sum_{i=1}^{M} \lambda_i f_i(u^*) = 0 \tag{3.16}$$

where M is any integer such that M>1. It is thus possible, subject to equation (3.16), to obtain systems of simultaneous independent equations from equations (3.3) and (3.4) by using any convenient number of functions from the set $f_i(u^*)$. At this point the choice of functional expressions for $f_i(u^*)$ is still arbitrary; the additional constraints which will be enforced in making a selection of a set of functions are determined from the following requirements:

(i) $f_i(u^*)$ should be a uniformly varying set of functions at least twice differentiable,

(ii) $f_i(u^*)$ should be such that the integrands in (3.3) and (3.4) can be evaluated without excessive labor, and

(iii) $f_i(u^*)$ should approach 0 as $u^* \to 1$ so that the first integral in (3.3) or (3.4) is bounded. This requirement occurs because $\rho^*\theta$ tends to infinity as u^* approaches unity.

Thus a satisfactory choice of $f_i(u^*)$ must satisfy the inequality

$$\lim_{u^* \to 1} \{f_i(u^*)\rho^*\theta\} < \infty \tag{3.17}$$

The inequality in equation (3.17) can be satisfied in a general way if the singularity associated with $\rho^*\theta$ in equation (3.11) is eliminated in the product of $f_i(u^*)$ and $\rho^*\theta$. If $f_i(u^*)$ is chosen as follows:

$$f_i(u^*) = (1-u^*)^i \; ; \; i = 1,2,\ldots,N \qquad (3.18)$$

then $f_i(u^*)$ satisfies all the required conditions. With increasing values of the exponent i, it is possible to accommodate higher order singularities of $\rho^*\theta$ as u^* approaches unity. These $f_i(u^*)$ given by equation (3.18) are monotonically decreasing functions of u^*. Equations (3.3) and (3.4) can now be integrated once the dependent variables $\rho^*\theta$ and h^*, and the weighting functions are replaced by the approximating and weighting functions derived in this section. It may be noted that because the coefficients a_i, b_i, c_i, and d_i are functions of ξ and τ only, the result of integrating equations (3.3) and (3.4) is a system of simultaneous partial differential equations involving these coefficients as the unknowns. In this study, the coefficients a_i, b_i, c_i and d_i are not derived solely from boundary conditions, they are also related to values of the dependent variables at points interior to the domain of interest, $(0<u^*<1)$. The derivation of expressions for these coefficients is described in Appendix A.

3.2 The Approximate System of Equations

Substitution of the approximating functions into the integro-differential equations yields 2N-1 partial differential equations obtained by using N functions in succession

from $f_i(u^*)$ in the reduced momentum equation, and N-1 functions in succession from $f_i(u^*)$ in the reduced energy equation. In particular, if the approximating function coefficients are chosen such that

$$\rho^*\theta \Big|_{u^*=i/N} = \rho_i\theta_i(\xi,\tau) \tag{3.19a}$$

$$h^* \Big|_{u^*=i/N} = h_i(\xi,\tau) \tag{3.19b}$$

$$Q \Big|_{u^*=i/N} = Q_i(\xi,\tau) \tag{3.19c}$$

for $i = 0, 1, 2 \ldots N-1$

then the resulting system of equations in 2N-1 unknowns are

$$\left(\rho_i\theta_i\right)^{\cdot} = \sum_{j=0}^{N-1} a_{ij}\left(\rho_j\theta_j\right)' + \sum_{j=0}^{N-1} \frac{b_{ij}}{\rho_j\theta_j} \tag{3.20}$$

$i = 0, 1, 2, \ldots N-1$

$$h_i = \sum_{j=1}^{N-1} c_{ij}\, h_j' + \sum_{j=0}^{N-1} d_{ij} h_j + \sum_{j=0}^{N-1} e_{ij} \tag{3.21}$$

$i = 1, 2, \ldots N-1$

in which N=1,2,3,..., and the dots over $\rho_i\theta_i$ and h_i indicate differentiation with respect to τ, while the primes over $\rho_i\theta_i$ and h_i represent differentiation with respect to ξ. The coefficients a_{ij}, b_{ij},c_{ij}, d_{ij} and e_{ij} are numbers or certain functions of $\rho_i\theta_i$, h_i and the transport properties ϕ_i and $(\phi/Pr)_i$. The boundary conditions associated with equations (3.20) and (3.21) are:

$$\rho_i\theta_i(\xi_s(\tau)) = 0 \tag{3.22a}$$

$$h_i(\xi_s(\tau)) = 1 \tag{3.22b}$$

The system (3.20) and (3.21) will be referred to in what follows as the approximating system in the N-th approximation. The system is closed and compatible in the sense that the approximating system has been derived from a well-posed problem. The coefficient h_0 in equation (3.21) is assumed known from the boundary condition at the wall in the form h_w = constant.

4. SOLUTION FOR N=1: FIRST APPROXIMATION

There are 2N-1 unknown parameters in the approximate system of equations (3.20) and (3.21), where N represents the order of the approximation. Since there are 2N-1 independent partial differential equations, N from (3.20) and N-1 from (3.21), solutions can be obtained for the functions $\rho_i\theta_i$ and h_i. In this section, an analytic solution will be obtained for the first approximation, N=1, and the result compared with the results of Mirels [1] and Lam and Crocco [4] for a perfect gas. In the next section, the second approximation will be obtained for both a perfect gas and a real gas.

The first approximation is obtained from equations (3.20) and (3.21) by setting N=1. The resulting equations are:

$$(\rho_o\theta_o)^{\cdot} = -\frac{1}{2}(\rho_o\theta_o)' + \frac{\phi_o}{\rho_o\theta_o} \tag{4.1}$$

$$h_o = \text{constant} \tag{4.2}$$

The boundary condition is

$$\text{at } \xi = \xi_s(\tau),\ \tau = \frac{U_e}{U_s}\xi_s : \rho_o\theta_o = 0 \tag{4.3}$$

Equations (4.1) and (4.2) are coupled in a trivial sense. Because the coefficient h_o is a constant from equation (4.2), the transport property ϕ_o is also constant. For this simple condition, it is possible to derive the following general

solution for equation (4.1):

$$\rho_o\theta_o(\xi,\tau) = \sqrt{\frac{4\phi_o}{2\alpha_1+\alpha_2}\,(\alpha_1\tau+\alpha_2\xi)} \tag{4.4}$$

Applying the boundary condition (4.3) yields:

$$\rho_0\theta_0(\xi,\tau) = \sqrt{\frac{4\phi_0}{\left(2\frac{U_s}{U_e}-1\right)}\left(\frac{U_s}{U_e}\,\tau - \xi\right)} \tag{4.5}$$

Note that it is not necessary to specify an initial condition on τ to obtain a solution for this problem. This is simply a result of the physical fact that time τ and distance ξ are trivially related by the stretched coordinate $U_s\tau/U_e - \xi$ appearing naturally in equation (4.5), another way of saying that in shock-fixed coordinates, the problem is steady.

From equation (3.13), the resulting enthalpy distribution becomes

$$h^*(\xi,u^*,\tau) = h_o + (1-h_o)\,u^*(\xi,\eta,\tau) \tag{4.6}$$

and the coefficient h_o is $h_o = h_w/h_e$.

The local skin friction coefficient is defined as

$$C_f = \frac{\left(\mu\,\frac{\partial u}{\partial y}\right)_{y=0}}{\rho_e U_e^{\,2}}$$

In the terminology of this report, the expression becomes:

$$C_f\,\sqrt{Re_x} = \frac{\phi_o\sqrt{\xi}}{\rho_o\theta_o} \tag{4.7}$$

where $Re_x = U_e x/\nu_e$. Equation (4.7) is an exact relation that holds for all orders of approximation. Substituting the analytic solution for the first approximation given by equation (4.5) yields the result:

$$C_f\sqrt{Re_x} = \sqrt{\frac{\left(2\,\frac{U_s}{U_e} - 1\right)\phi_0}{4\left(\frac{U_s}{U_e}\,\frac{\tau}{\xi} - 1\right)}} \tag{4.8}$$

As a part of their analysis, Lam and Crocco [4] solved for the boundary-layer flow behind a moving plane shock wave assuming a perfect gas (they also considered the leading-edge problem). On the basis of their results, Lam and Crocco suggested a modification of an expression derived by Mirels [1] for the skin-friction coefficient. Mirels' expression, as modified by Lam and Crocco can be written in the form:

$$C_f\sqrt{Re_x} = \sqrt{\frac{2.82\,\frac{U_s}{U_e} - 1}{6\left(\frac{U_s}{U_e}\,\frac{\tau}{\xi} - 1\right)}} \tag{4.9}$$

Equations (4.8) and (4.9) are compared in Figure 2 for a perfect gas ($\phi_o = 1$). The agreement between these two results is within six percent over the total range shown.

The enthalpy profile given by equation (4.6) is compared with Mirels' [1] results in Figure 3. In this figure, Mirels' similarity variable η_m is defined as

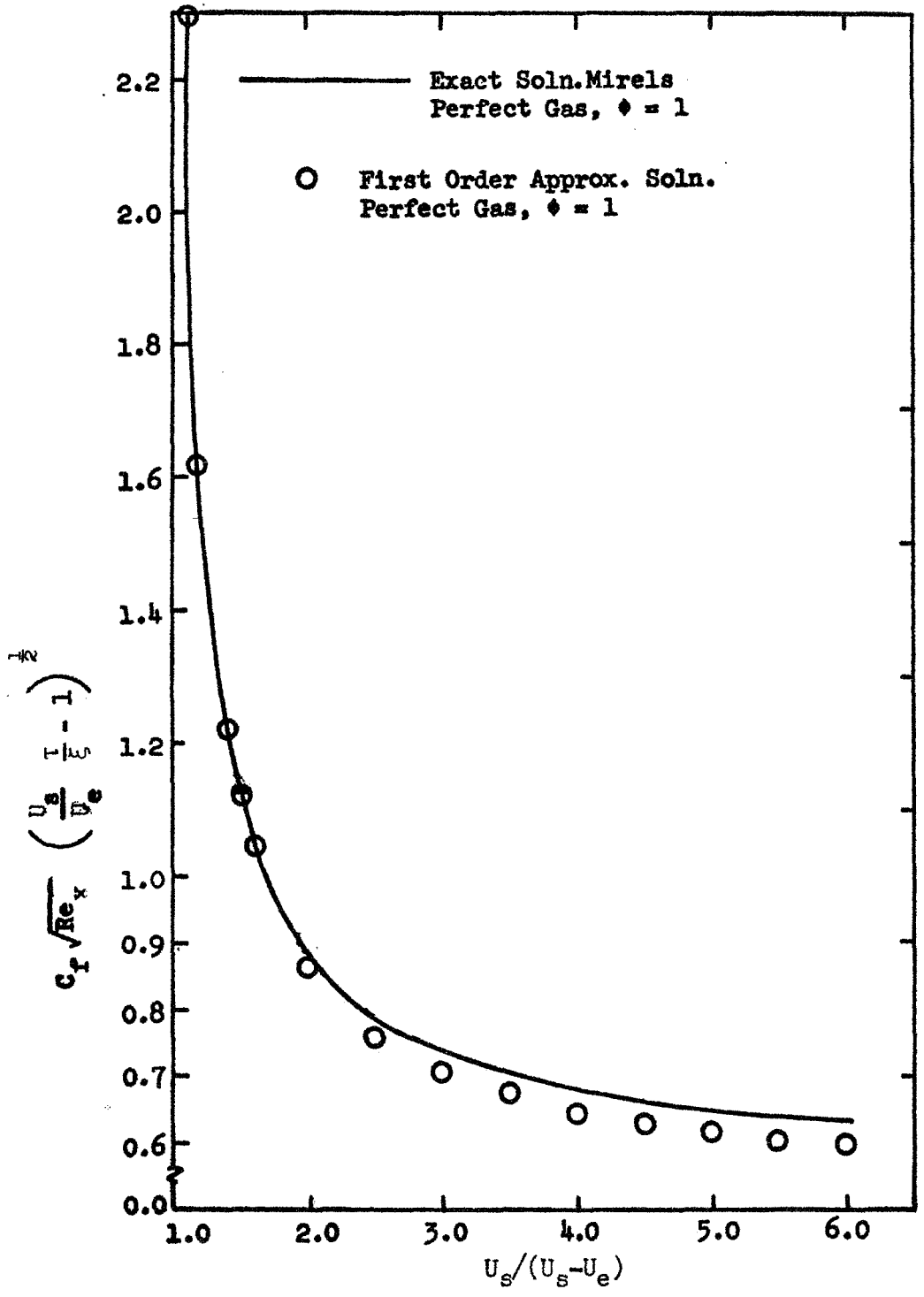

Figure 2. Comparison of First Order Approximate Solution with Exact Solution of Mirels [1] as modified by Lam and Crocco [4].

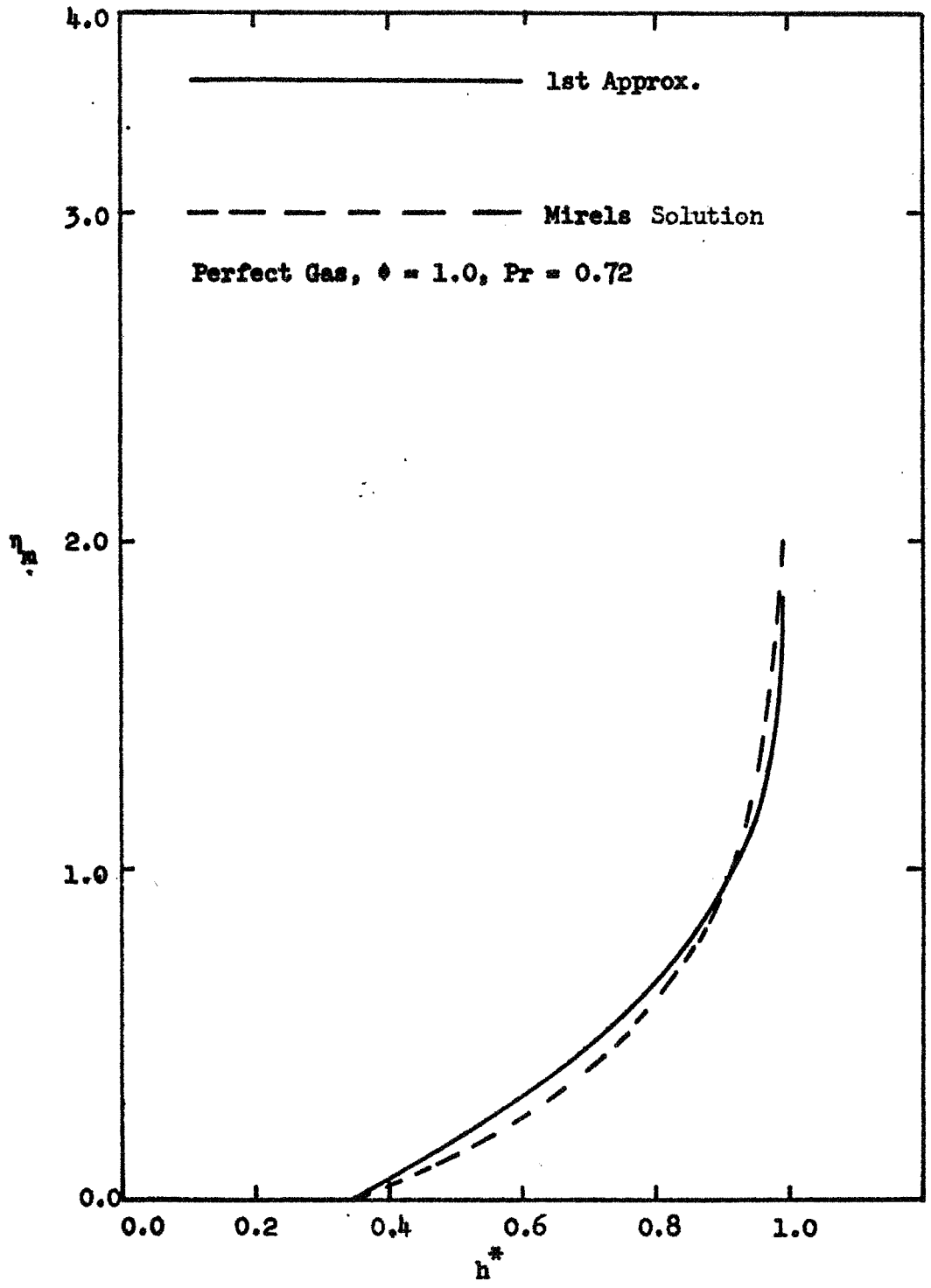

Figure 3. Comparison of Enthalpy Profile with Mirels' [1] Solution.

a. w = 4

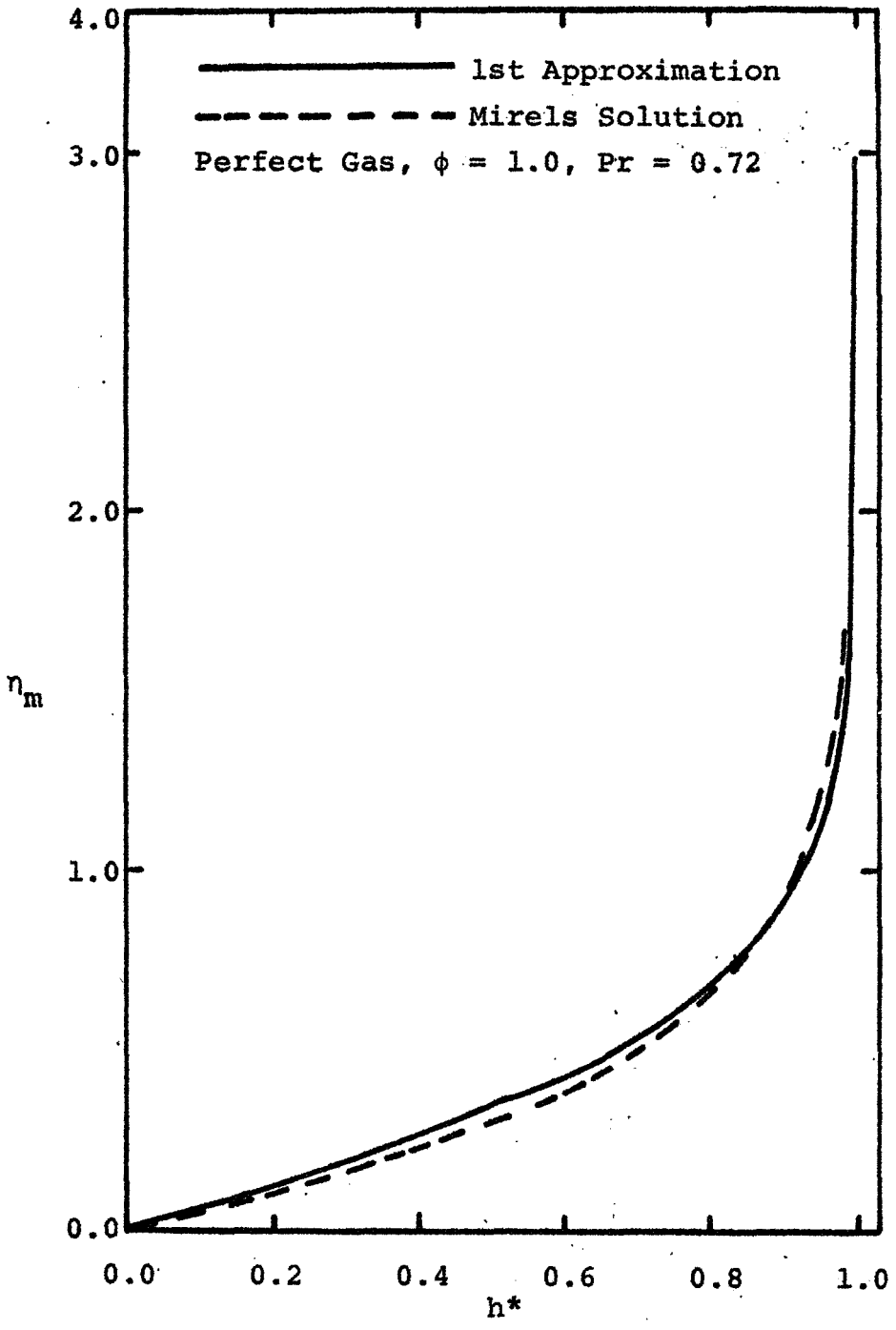

Figure 3. Comparison on Enthalpy Profile with Mirels' [1] Solution.

b. w = 6

$$\eta_m = \sqrt{\frac{\hat{U}_e}{2\hat{x}\nu_w}} \int_0^y \frac{\rho}{\rho_w}\, dy \tag{4.10}$$

where

$$\hat{x} = U_s t - x \tag{4.11}$$

and

$$\hat{U}_e = U_s - U_e \tag{4.12}$$

Mirels' variable η_m is related to h* through u* by equation (4.6), and u* is related to y by the definition of θ:

$$\frac{y}{L}\sqrt{\frac{U_e L}{\nu_e}} = \int_0^{u^*} \theta\, du^* \tag{4.13}$$

(note that $\rho^* = 1/h^*$ for a perfect gas across a boundary layer). The parameter w is the velocity ratio across a stationary shock wave, given by

$$w = \frac{U_s}{U_s - U_e} = \frac{U_s}{\hat{U}_e} \tag{4.14}$$

The figure shows that the MWR first approximation is remarkably accurate for such a low order approximation. It would thus be anticipated that a second approximation would give very adequate engineering accuracy; this expectation is verified in the next section.

5. SOLUTION FOR N=2: SECOND APPROXIMATION

In the last section, a solution for $\rho^*\theta$ for a first MWR approximation was obtained which contained one free parameter $\rho_o^*\theta_o$, while the enthalpy function h* contained no free parameters, depending only on the wall condition and conditions at the outer edge of the boundary layer. Specifically, the first approximation took the form:

$$N=1: \quad \rho^*\theta \simeq \frac{\rho_o\theta_o}{1-u^*} \tag{5.1a}$$

$$h^* \simeq h_o + (1-h_o)\, u^* \tag{5.1b}$$

where $h_o = h_w/h_e$, a constant. The utility of this approximation, aside from the remarkably good accuracy obtained for a one-parameter approximation, is the fact that an analytical solution was possible and questions concerning a numerical treatment of partial differential equations did not enter the analysis. In the present section, the second MWR approximation will be derived in plate-fixed coordinates. The resultant set of reduced equations is the form that must be solved for a truly unsteady problem, and this is the form treated in the companion report where the plate leading edge is considered. However, for the present case of the boundary layer behind a plane shock wave, the corresponding shock-fixed coordinates will be reverted to and the resulting second approximation

results compared with Mirels' [1] enthalpy distributions for a perfect gas. This analytical approach allows the attendant numerical difficulties of solving partial differential equations in two independent variables to be delayed until the basic MWR technique is well established.

For a second approximation, the integro-differential equations (3.20) and (3.21) will contain two free parameters for the $\rho^*\theta$-function and one free parameter for the h^*-function. The appropriate approximations are given by:

$$N=2: \qquad \rho^*\theta \simeq \frac{1}{1-u^*}\left[(1-2u^*)\,\rho_o\theta_o + u^*\rho_1\theta_1\right] \tag{5.2a}$$

$$h^* \simeq a_o + a_1 u^* + a_2 u^{*2} \tag{5.2b}$$

where

$$a_o = h_o = h_w/h_e \tag{5.3a}$$

$$a_1 = -3h_o + 4h_1 - 1 \tag{5.3b}$$

$$a_2 = 2h_o - 4h_1 + 2 \tag{5.3c}$$

The detailed derivation of equations (5.3) is given in Appendix A. Introducing the approximation (5.2a) into equation (3.20) for N=2 yields the two equations, in matrix form

$$\begin{bmatrix} (\rho_o\theta_o)^{\cdot} \\ (\rho_1\theta_1)^{\cdot} \end{bmatrix} = \begin{bmatrix} -1/3 & 1/6 \\ 1/3 & -2/3 \end{bmatrix} \begin{bmatrix} (\rho_o\theta_o)' \\ (\rho_1\theta_1)' \end{bmatrix} + \begin{bmatrix} 8 & -8 \\ 2 & 0 \end{bmatrix} \begin{bmatrix} \dfrac{\phi_o}{\rho_o\theta_o} \\ \dfrac{\phi_1}{\rho_1\theta_1} \end{bmatrix} \tag{5.4}$$

Also, substituting equation (5.2) into equation (3.21) with N=2 yields the equation

$$\frac{\partial h_1}{\partial \tau} = \Bigg[-a_0 \frac{(\rho_0\theta_0)^{\cdot}}{2} - a_1\left\{-\frac{1}{6}(\rho_0\theta_0)^{\cdot} + \frac{1}{3}(\rho_1\theta_1)^{\cdot}\right\}$$

$$-a_2\left\{-\frac{1}{6}(\rho_0\theta_0)^{\cdot} + \frac{1}{4}(\rho_1\theta_1)^{\cdot}\right\} - \left(-\frac{1}{15}\rho_0\theta_0 + \frac{1}{5}\rho_1\theta_1\right)\frac{\partial h_1}{\partial \xi}$$

$$-a_0\left\{-\frac{1}{6}(\rho_0\theta_0)' + \frac{1}{3}(\rho_1\theta_1)'\right\} - a_1\left(-\frac{1}{6}(\rho_0\theta_0)' + \frac{1}{4}(\rho_1\theta_1)'\right)$$

$$-a_2\left\{-\frac{3}{20}(\rho_0\theta_0)' + \frac{1}{5}(\rho_1\theta_1)'\right\} - a_1\left(\frac{\phi}{Pr}\right)_0 \frac{1}{\rho_0\theta_0} + a_0\frac{\phi_0}{\rho_0\theta_0}$$

$$+a_1\left\{\frac{1}{6}\frac{\phi_0 + \left(\frac{\phi}{Pr}\right)_0}{\rho_0\theta_0} + \frac{2}{3}\frac{\phi_1 + \left(\frac{\phi}{Pr}\right)_1}{\rho_1\theta_1}\right\} + \frac{2}{3}a_2\frac{\phi_1 + \left(\frac{\phi}{Pr}\right)_1}{\rho_1\theta_1}$$

$$+\frac{U_e^2}{g_c J h_e}\left(\frac{1}{6}\frac{\phi_0}{\rho_0\theta_0} + \frac{1}{3}\frac{\phi_1}{\rho_1\theta_1}\right)\Bigg] \Bigg/ \left(\frac{3}{\rho_1\theta_1}\right) \qquad (5.5)$$

The appropriate boundary conditions become:

$$\rho_i\theta_i\ (\xi_s,\tau) = 0 \quad \text{for } i=0,1 \qquad (5.6a)$$

$$h_1\ (\xi_s,\tau) = 1 \qquad (5.6b)$$

The dots again represent differentiation with respect to τ and the primes differentiation with respect to ξ.

In the reduced momentum equation, (5.4), it will be seen that in addition to introducing the free parameter $\rho_1\theta_1$, a new term ϕ_1 has appeared in the system of equations. Recall that ϕ_i has been defined as

$$\phi_i = \phi\Big|_{u^*=i/N} \qquad (5.7)$$

where i=0, 1 and N=2 in the scheme of the second approximation. In the energy equation (5.5), h_1 is a dependent variable occurring in addition to the h_o term. Similar to equation (5.7) the functional group $(\phi/Pr)_i$ appearing in the energy equation is defined by

$$\left(\frac{\phi}{Pr}\right)_i = \left(\frac{\phi}{Pr}\right)_{u^*=i/N} \tag{5.8}$$

where i=0, 1 and N=2. In general ϕ_i and $(\phi/Pr)_i$ are functions of the enthalpy field within the boundary layer, thus it is clear that equations (5.4) and (5.5) are coupled through these terms. Remember that in the system of equations under the first approximation, equations (4.1) and (4.2), a coupling exists between the momentum and the energy equations in a trivial sense only. Because h_o is a constant, it follows that ϕ_o is constant for all orders of approximation.

The dependence of ϕ_1 on ξ and τ is not known a priori for the general case of a real gas; its variation will depend on the appropriate thermodynamic relations and will depend implicitly on the solution for h*. However, if a perfect gas is assumed and ϕ_1 is a constant (but not necessarily equal to ϕ_o or unity), equations (5.4) and (5.5) are uncoupled and equation (5.4) has an analytic solution given by

$$\rho_i\theta_i = A_i \sqrt{\frac{U_s}{U_e}\tau - \xi} \tag{5.9}$$

It is seen that the argument of equation (5.9) is the same "elapsed-time" or "quasi-steady" variable that was found for the first approximation. The coefficients A_i are constants that may be found by iteration from equation (5.4).

When the thermodynamic variable ϕ_1 is allowed to vary continuously as it does for a real gas, equations (5.4) and (5.5) are coupled and equation (5.9) is no longer a solution. Thus, numerical techniques for solving partial differential

equations must be employed to obtain solutions. In a companion report, finite difference numerical techniques are employed to solve these equations which allow not only for real gas property variations but also truly unsteady effects. However, for the present work finite difference methods will be avoided by converting the governing equations to shock-fixed coordinates, a step which automatically reduces the problem to a single independent variable. The resulting equations will then be solved by standard numerical techniques for ordinary differential equations.

5.1 Shock-Fixed Formulation

The dependent and independent variables in the shock-fixed and plate-fixed coordinate systems are related as follows

$$\hat{x} = U_s t - x \tag{5.10a}$$

$$\hat{y} = y \tag{5.10b}$$

$$\hat{u} = U_s - u \tag{5.10c}$$

$$\hat{v} = v \tag{5.10d}$$

in which the diacritical sign [i.e.(^)] represents the shock-fixed system. Note that in the $(\hat{x},\hat{y})$-system, the wall moves at the speed of the shock U_s, and in this coordinate system the flow is steady. Defining nondimensional variables in the shock-fixed reference system by

$$\hat{\xi} = \frac{\hat{x}}{L} \tag{5.11a}$$

$$\hat{\eta} = \sqrt{\hat{Re}_L}\,\frac{\hat{y}}{L} \tag{5.11b}$$

$$u^{**} = \frac{\hat{u}}{\hat{U}_e} \tag{5.11c}$$

where the Reynolds number is defined by

$$\hat{Re}_L = \frac{\rho_e \hat{U}_e L}{\mu_e}$$

(where $\hat{U}_e = U_s - U_e$) and the related inverse velocity gradient variable by

$$\hat{\theta} = \left(\frac{\partial u^{**}}{\partial \hat{\eta}}\right)^{-1} \tag{5.12}$$

the integro-differential equations in (3.3) and (3.4) take the form

$$\frac{\partial}{\partial \hat{\xi}} \int_w^1 f_i(u^{**}) \rho^* \hat{\theta} u^{**} du^{**} = -\left(f_i(u^{**}) \frac{\phi}{\rho^* \hat{\theta}} \right)_{u^{**}=w} - \int_w^1 f_i''(u^{**}) \frac{\phi}{\rho^* \hat{\theta}} du^{**} \tag{5.13}$$

$$\frac{\partial}{\partial \hat{\xi}} \int_w^1 f_i(u^{**}) h^* \rho^* \hat{\theta} u^{**} du^{**} = -\left(f_i(u^{**}) \frac{\partial h^*}{\partial u^{**}} \frac{\phi}{Pr} \frac{1}{\rho^* \hat{\theta}} \right)_{u^{**}=w} - \left(f_i'(u^{**}) h^* \frac{\phi}{\rho^* \hat{\theta}} \right)_{u^{**}=w} - \int_w^1 \left(\phi + \frac{\phi}{Pr}\right) \frac{\partial h^*}{\partial u^{**}} \frac{f_i(u^{**})}{\rho^* \hat{\theta}} du^{**} \cdot$$

$$- \int_w^1 h^* f_i''(u^{**}) \frac{\phi}{\rho^* \hat{\theta}} du^{**} + \frac{\hat{U}_e^2}{g_c J h_e} \int_w^1 \frac{\phi}{\rho^* \hat{\theta}} f_i(u^{**}) du^{**} \tag{5.14}$$

The freestream velocity $\hat{U}_e$ is taken from the normal shock tables, and w is the ratio $U_s/\hat{U}_e$, of the velocity ahead of and behind the stationary normal shock. The boundary

conditions associated with (5.13) and (5.14) are:

$$\rho_i^* \hat{\theta}_i (\hat{\xi}=0) = 0 \tag{5.15a}$$

$$h^*(\hat{\xi}=0, u^{**} \neq w) = 1 \tag{5.15b}$$

As discussed in Section 3.1, the weighting and approximating functions associated with $f_i(u^{**})$ and $\rho^* \hat{\theta}$ must satisfy the proper physical characteristics. Now, however, the approximation functions are formulated with a nonzero velocity at $\eta = 0$. Also, the inverse velocity function $\hat{\theta}$ is now negative because the highest flow velocity occurs at the wall and decays monotonically across the boundary layer to the value $\hat{U}_e$ at the outer edge.

The approximating functions are also derived in Appendix A for shock-fixed coordinates. They take the form:

$$\rho^* \hat{\theta} \simeq \frac{1}{1-u^{**}} \left[(w+1-2u^{**}) \rho_o \hat{\theta}_o + (u^{**}-w) \rho_1 \hat{\theta}_1 \right] \tag{5.16}$$

$$\frac{Q}{\rho^* \hat{\theta}} \simeq \frac{1-u^{**}}{(1-w)^2} \left[(w+1-2u^{**}) \frac{Q_o}{\rho_o \hat{\theta}_o} + 4(u^{**}-w) \frac{Q_1}{\rho_1 \hat{\theta}_1} \right] \tag{5.17}$$

$$h^* \simeq \frac{1}{(1-w)^2} \left[(w+1) h_o - 4w h_1 + w(w+1) + [-(3+w) h_o + 4(w+1) h_1 - (1-3w)] u^{**} + (2h_o - 4h_1 + 2) u^{**2} \right] \tag{5.18}$$

The approximation functions preserve the characteristic listed previously. The free parameters are obtained from

$$\psi_i = \psi \Big|_{u^{**}=i/N} \tag{5.19}$$

where i=0, 1, and

$$\psi \equiv \begin{cases} \rho^*\hat{\theta} \\ h^* \\ \dfrac{Q}{\rho^*\hat{\theta}} \end{cases} \qquad (5.19b)$$

and

$$Q \equiv \begin{cases} \phi \\ \dfrac{\phi}{Pr} \text{ or } \left(\phi + \dfrac{\phi}{Pr}\right) \end{cases} \qquad (5.19c)$$

The weighting function is taken to be

$$f_i(u^{**}) = (1-u^{**})^i$$
$$i=1,2,\ldots N \qquad (5.20)$$

Substitution of these approximating and weighting functions into the integro-differential equations (5.13) and (5.14) leads routinely to the following differential equations:

$$A_{ij} \begin{bmatrix} (\rho_o\hat{\theta}_o)' \\ (\rho_1\hat{\theta}_1)' \end{bmatrix} = B_{ij} \begin{bmatrix} \dfrac{\phi_o}{\rho_o\hat{\theta}_o} \\ \dfrac{\phi_1}{\rho_1\hat{\theta}_1} \end{bmatrix} \qquad (5.21)$$

where the elements of the matrix A_{ij} are

$$a_{11} = (w+1)(1-w^2)/2-2(1-w^3)/3$$

$$a_{12} = (1-w^3)/3-w(1-w^2)/2$$

$$a_{21} = (w+1)[(1-w^2)/2-(1-w^3)/3]-2(1-w^3)/3+2(1-w^4)/4$$

$$a_{22} = (1-w^3)/3-(1-w^4)/4-w[(1-w^2)/2-(1-w^3)/3]$$

and the elements of the matrix B_{ij} are

$$b_{11} = 1$$

$$b_{12} = 0$$

$$b_{21} = 2(1-w)-2\left[(w+1)[1-w-(1-w^2)/2]-(1-w^2)/2+(1-w^3)/3\right]/(1-w)^2$$

$$b_{22} = 8\left[(1-w^2)/2-(1-w^3)/3-w[1-w-(1-w^2)/2]\right]/(1-w)^2$$

The energy equation is obtained as:

$$\frac{\partial h_1}{\partial \xi} = (RHS-LHS)/AH \tag{5.22}$$

where

$$RHS = RHS\left[\rho_0\hat{\theta}_0, \rho_1\hat{\theta}_1, w, h_0, h_1, \phi_i, \left(\frac{\phi}{Pr}\right)_i\right]$$

$$LHS = LHS\left[\rho_0\hat{\theta}_0, \rho_1\hat{\theta}_1, w, h_0, h_1, \phi_i, \left(\frac{\phi}{Pr}\right)_i\right]$$

$$AH = AH\left(w, \rho_0\hat{\theta}_0, \rho_1\hat{\theta}_1\right)$$

The derivations for RHS, LHS, AH are shown in Appendix B.

The boundary conditions associated with (5.21) and (5.22) are:

$$\rho_0\hat{\theta}_0(\hat{\xi}=0) = 0 \tag{5.23a}$$

$$\rho_1\hat{\theta}_1(\hat{\xi}=0) = 0 \tag{5.23b}$$

$$h_1(\hat{\xi}=0) = 1 \tag{5.23c}$$

The solution of equations (5.21) and (5.22) with boundary conditions (5.23) will now be separately discussed for a perfect gas with ϕ = constant and for a real gas (nitrogen).

5.2 Perfect Gas Solution

The matrix A_{ij} is nonsingular. Upon assuming a perfect gas and setting $\phi_i = 1$, equation (5.21) may be inverted to give

$$\begin{bmatrix} (\rho_o\hat{\theta}_o)' \\ (\rho_1\hat{\theta}_1)' \end{bmatrix} = E_{ij} \begin{bmatrix} \frac{1}{\rho_o\hat{\theta}_o} \\ \frac{1}{\rho_1\hat{\theta}_1} \end{bmatrix} \tag{5.24}$$

where $E_{ij} = A_{ij}^{-1} B_{ij}$ in which A_{ij}^{-1} is the unique inverse of the matrix A_{ij}. The energy equation depends on both ϕ_i and $(\phi/Pr)_i$. Choosing ϕ=1 and setting Pr=0.72 (a constant) the elements of equation (5.22) take the form:

$$RHS = RHS(\rho_o\hat{\theta}_o, \rho_1\hat{\theta}_1, w, h_o, h_1, Pr) \tag{5.25a}$$

$$LHS = LHS(\rho_o\hat{\theta}_o, \rho_1\hat{\theta}_1, w, h_o, h_1, Pr) \tag{5.25b}$$

$$AH = AH(\rho_o\hat{\theta}_o, \rho_1\hat{\theta}_1) \tag{5.25c}$$

The derivation of the above equations follows directly from the more general results given in Appendix B. The boundary conditions given by equation (5.23) are unchanged.

The integration of equations (5.22) and (5.24) with boundary conditions (5.23) was achieved by standard numerical computation on an IBM 7094 computer using an Adam-Moulton variable step-size routine. The error margin during computation was set so as to be dynamically related to the current growth characteristics of $\rho_o\hat{\theta}_o$, $\rho_1\hat{\theta}_1$ and h_1, thus assuring a small error in the fifth decimal place. Since the upper limit of $\hat{\xi}$ is unbounded in the context of the present problem, it was varied from zero to an arbitrary value of unity.

Upon substituting the numerical solutions for the parameters $\rho_o\hat{\theta}_o$, $\rho_1\hat{\theta}_1$, and h_1 obtained from equations (5.24) and (5.25) into the approximations for $\rho^*\hat{\theta}$ and h^* given by equations (5.16), (5.17), and (5.18), the standard boundary-layer parameters may be computed from the following definitions:

Skin-friction coefficient:

$$\hat{C}_f \sqrt{\hat{Re}_L} = \frac{\phi_o}{\rho_o \hat{\theta}_o} \tag{5.26a}$$

Velocity profile:

$$\frac{Y}{L} \sqrt{\hat{Re}_L} = \int_w^{u^{**}} \hat{\theta}\, du^{**} \tag{5.26b}$$

Boundary-layer thickness:

$$\frac{\delta}{L} \sqrt{\hat{Re}_L} = \int_w^{U_e^{**}} \hat{\theta}\, du^{**} \tag{5.26c}$$

Displacement thickness:

$$\frac{\delta^*}{L} \sqrt{\hat{Re}_L} = \int_w^{U_e^{**}} \hat{\theta}(1-\rho^* u^{**})\, du^{**} \tag{5.26d}$$

Momentum Thickness:

$$\frac{\delta^{**}}{L} \sqrt{\hat{Re}_L} = \int_w^{U_e^{**}} \rho^* \hat{\theta} u^{**}(1-u^{**})\, du^{**} \tag{5.26e}$$

Energy dissipation thickness:

$$\frac{\delta^{***}}{L} \sqrt{\hat{Re}_L} = \int_w^{U_e^{**}} \rho^* \hat{\theta} u^{**}(1-u^{**2})\, du^{**} \tag{5.26f}$$

Nusselt number:

$$\frac{Nu(1-h_o)}{\hat{Re}_L} = \frac{1}{\hat{\theta}_o} \left(\frac{\partial h^*}{\partial u^{**}} \right)_{u^{**}=w} \tag{5.26g}$$

The relation between these parameters and the conventional definitions for a plate-fixed coordinate system is given in Appendix D. Note that for a perfect gas with constant specific heats ρ^* is related to h^* across the boundary layer

by the simple relation $\rho^* = 1/h^*$.

Calculations were made for $2 \leq w \leq 6$ with $\phi = 1$ and $Pr = 0.72$ and the results are given in Tables 1 and 2. Typical results for the skin-friction coefficient, velocity profiles, and enthalpy profiles are shown in Figures 4, 5, and 6, respectively. The present results for the enthalpy profiles are compared with Mirels' [1] calculations in Figure 7 (note the change in scale of the abscissa at u**=2); this comparison shows agreement within 3 percent or better for all the values of w. The present calculations for the boundary-layer parameters are in excellent agreement with those of Mirels [1]. For example, it is found that the skin-friction coefficient calculations agree within better than a percent over the entire range of the present calculations.

It is now of interest to consider the solution of equations (5.21) and (5.22) where the thermodynamic and transport property parameters are related to real gas variations for nitrogen. By gaining confidence in the accuracy of the MWR second approximation through the above comparison with Mirels' [1] solutions for a perfect gas, it will then prove possible to draw certain conclusions regarding perfect gas and real gas behavior.

5.3 Real Gas Solution

Equations (5.21), (5.22), and (5.23) were also solved assuming a real gas in thermodynamic equilibrium. Nitrogen was selected as the gas for these calculations with the thermodynamic and transport properties being taken from

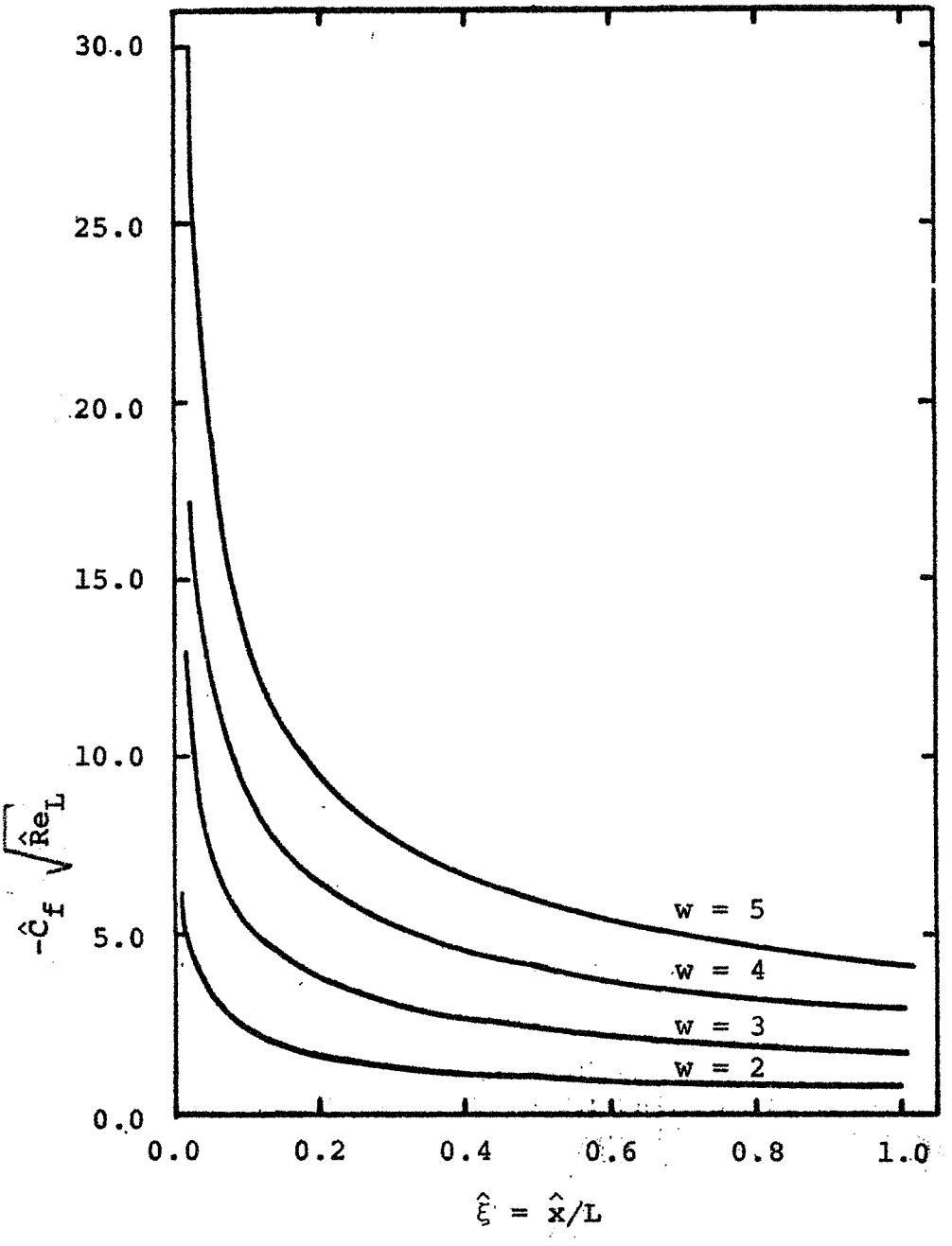

Figure 4. Skin Friction Coefficient Variation, Perfect Gas Solution, Second Approximation.

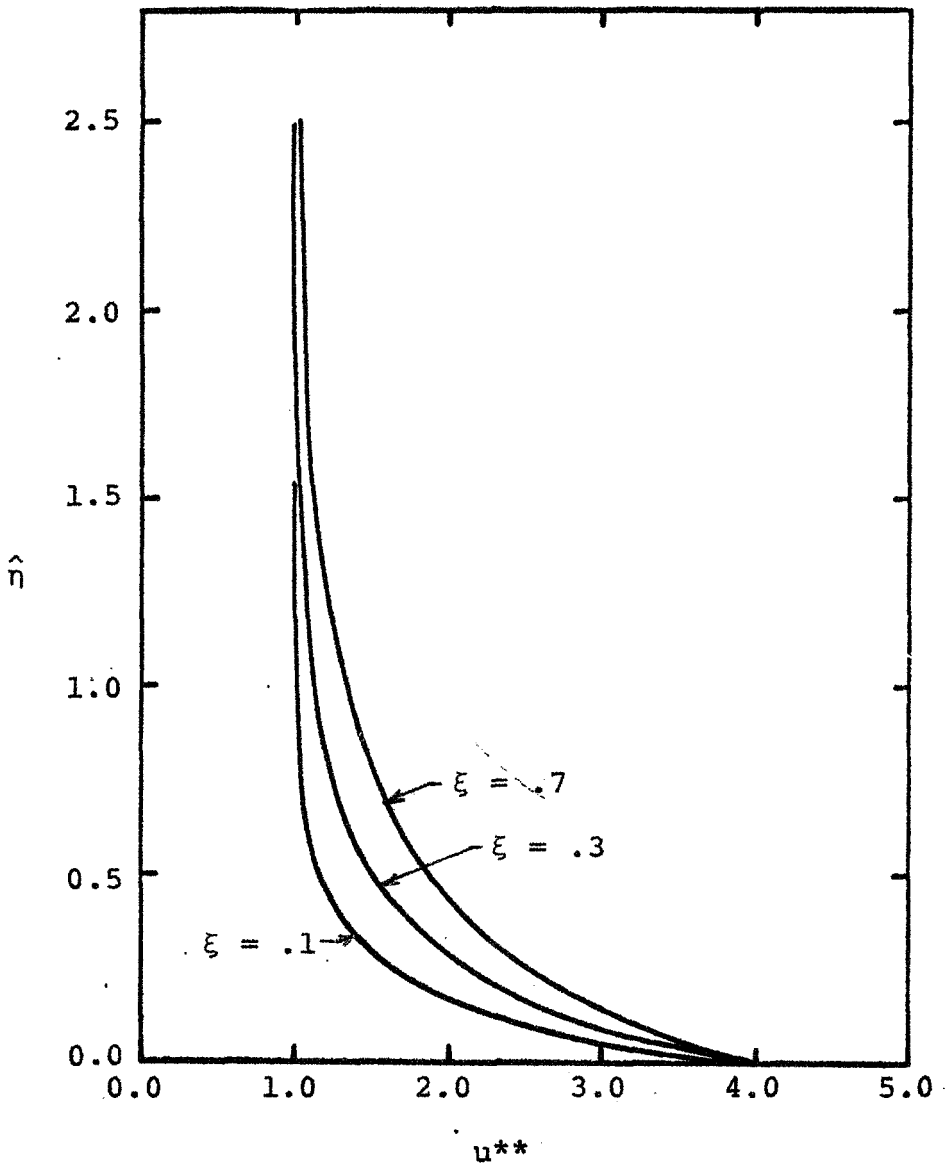

Figure 5. Typical Velocity Profiles, Perfect Gas Solution, w = 4, Second Approximation.

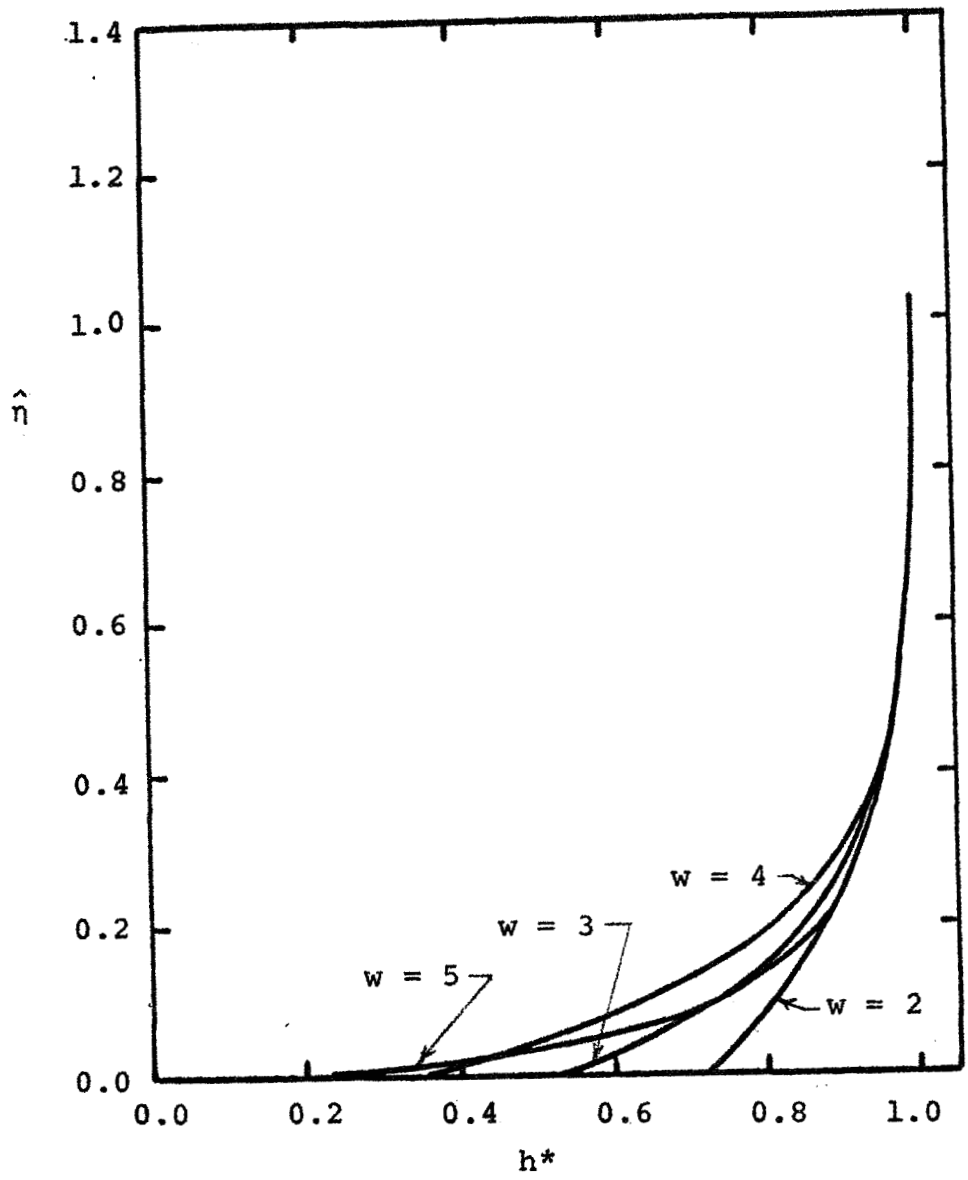

Figure 6. Enthalpy Profile at $\xi = 0.1$ for Perfect Gas Solution, Second Approximation.

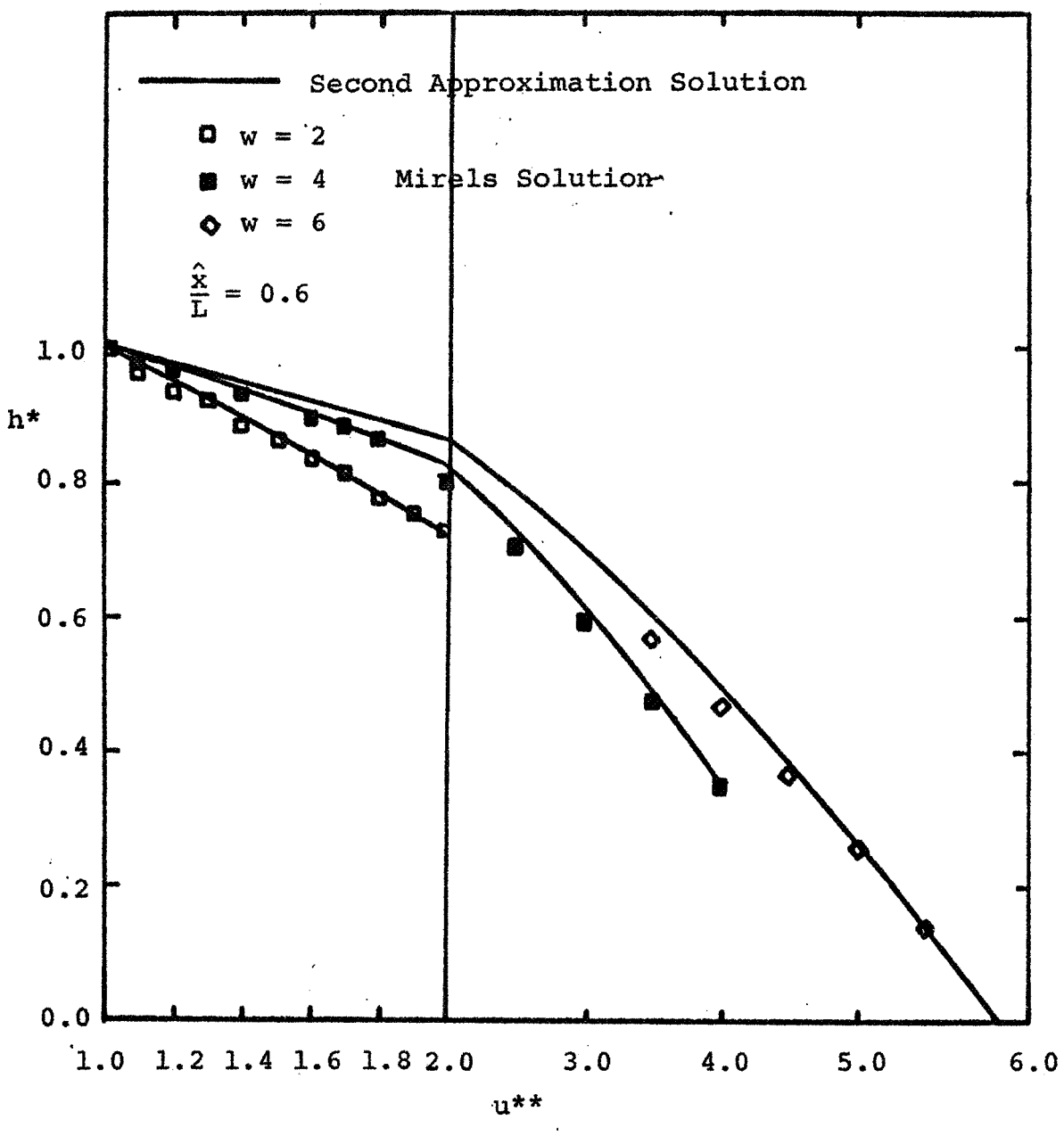

Figure 7. Comparison of Enthalpy Profile with Mirels' [1] Solution for Perfect Gas, Second Approximation.

Ahtye and Peng [14] as curve fit by Marvin and Deiwert [15]. Results were obtained assuming an initial pressure of 0.001 atm and an initial temperature of 530°R. The values of ϕ and ϕ/Pr as a function of h/h_r are obtained from the property polynomials given in Appendix C. The reference enthalpy h_r is given in Table C-1. The real gas properties are related to the approximation functions ϕ_i and $(\phi/Pr)_i$ by equations (5.7) and (5.8), and the values of enthalpy ratio used for evaluating these variables are obtained from equation (3.19b) together with the following expression

$$\frac{h}{h_r} = \frac{h_e}{h_r} h_i^* \quad ; \quad i=0,1,\ldots N-1 \tag{5.27}$$

The numerical calculations were again obtained on an IBM 7094 digital computer using an Adam-Moulton numerical method.

The boundary-layer parameters defined by equations (5.26) were calculated for various values of the shock wave parameter w and the results are given in Table 3. The variation of skin-friction coefficient and Nusselt number with $\hat{\xi}$ is shown in Figures 8 and 9, respectively. On comparing Figure 8 with Figure 4, it is seen that there is considerable departure from the perfect gas calculations for the skin-friction coefficient. For example, at w = 6 and $\hat{\xi} = 1$, there is a four-fold increase in the nondimensional skin-friction when the real gas properties are used. By reference to Tables 1c and 3c, it is seen that the numerical values of $\rho_o \hat{\theta}_o$ differ by less than 0.2 percent. The large real gas variation in the skin-friction coefficient is, rather, accounted for by the

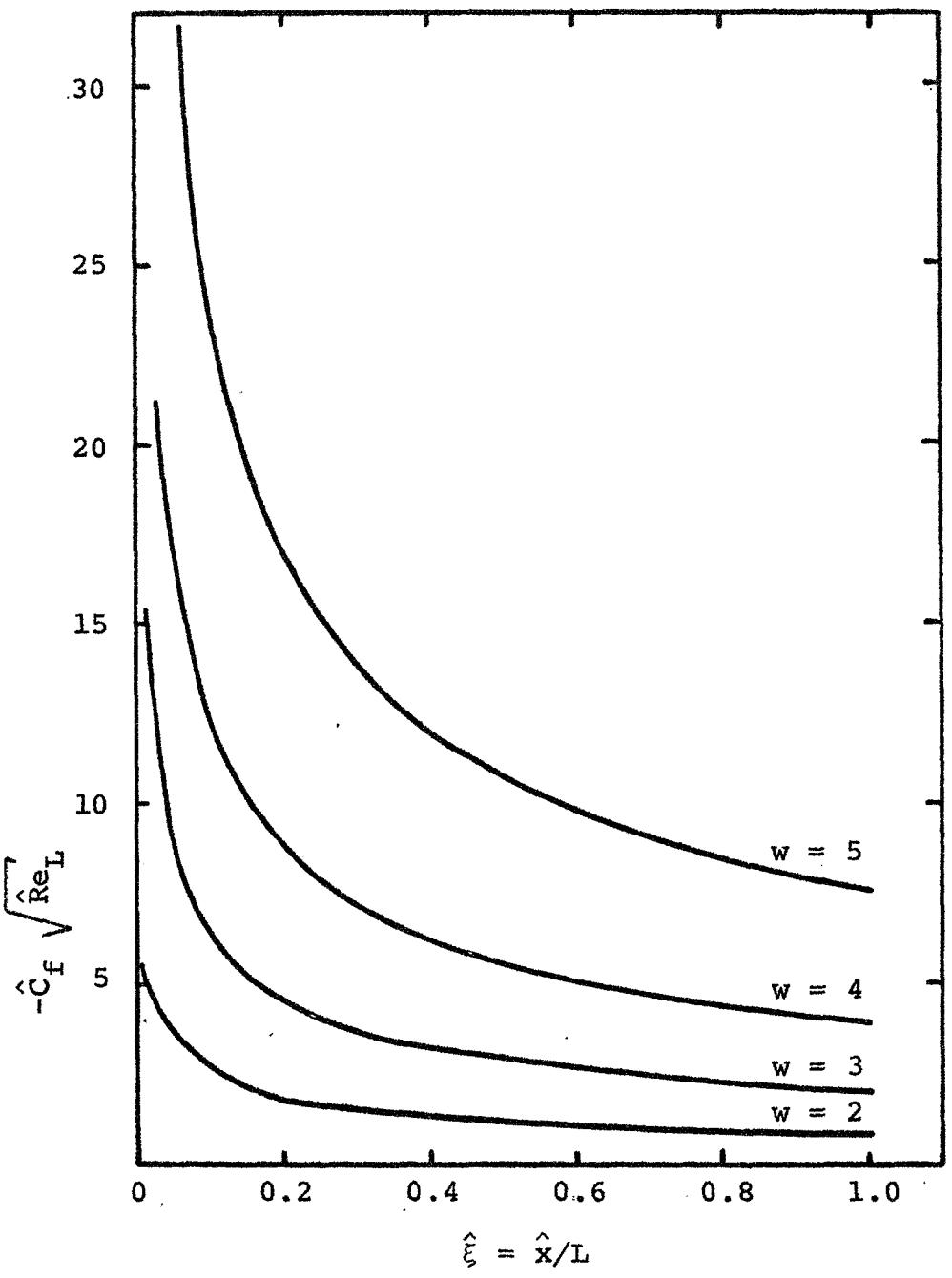

Figure 8. Skin Friction Coefficient Variation, Real Gas Solution, Second Approximation.

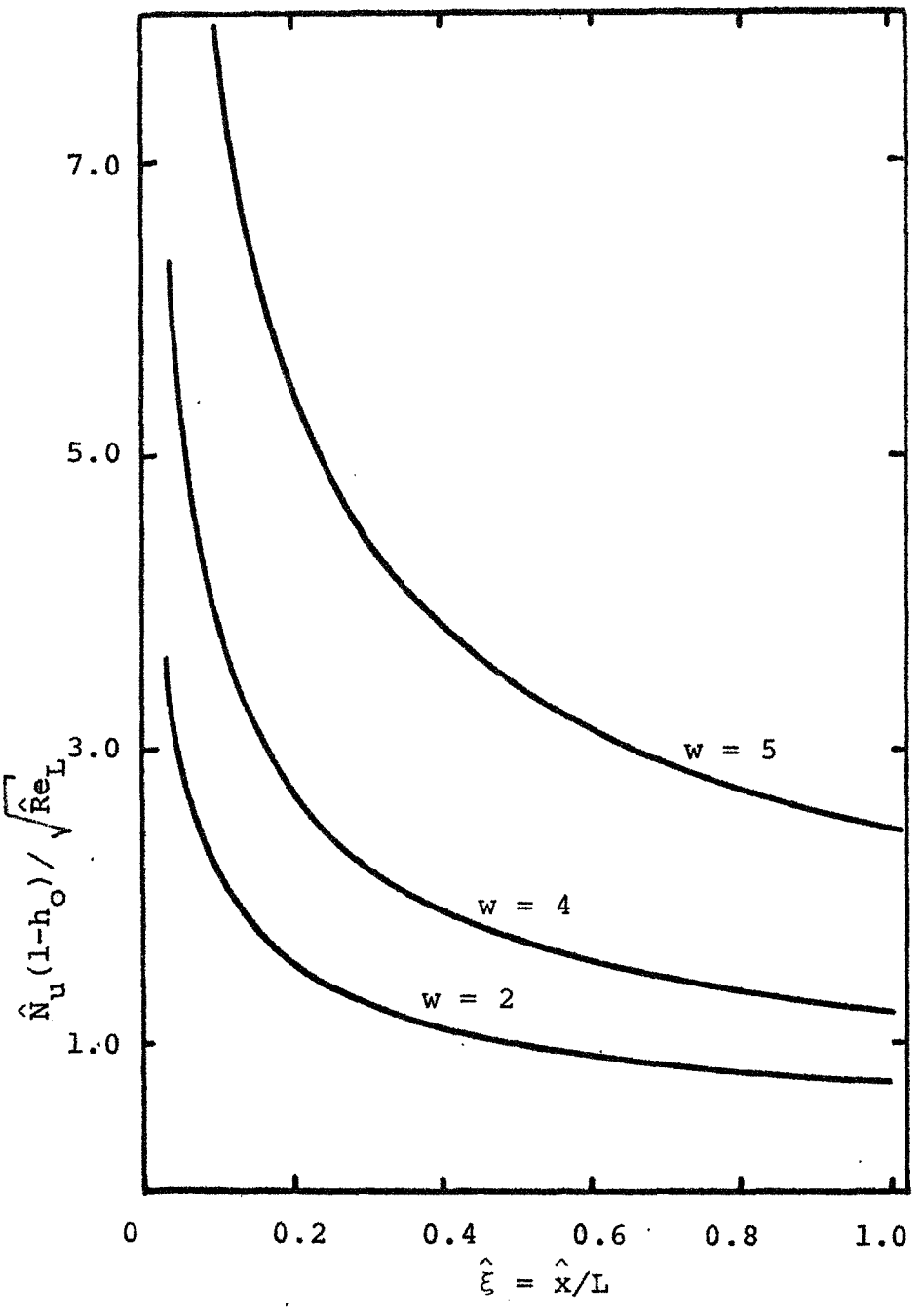

Figure 9. Variation of Heat Transfer Parameter, Real Gas Solution, Second Approximation.

variation in the ϕ_o as shown in Figure 10. It is seen in this figure that ϕ_o is increasing in a exponential fashion with increasing w.

Comparison of the values given in Tables 1 and 3 show that, except at w = 2, the boundary-layer thicknesses are somewhat smaller for a real gas. Typical enthalpy profiles for both the real and perfect gas solutions are shown in Figure 11. In general, the real gas departure from the perfect gas model increases for all of the computed quantities, as expected, as the shock strength increases.

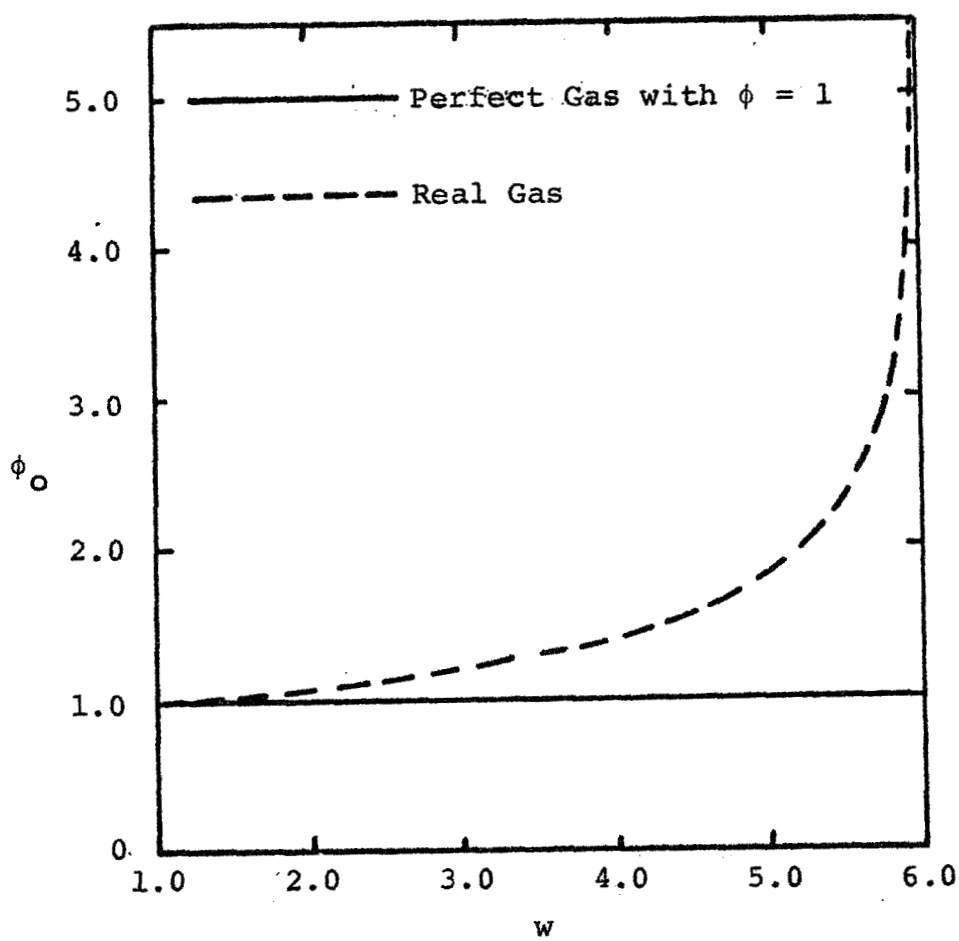

Figure 10. Dependence of ϕ_o on Shock Intensity Parameter, Second Approximation.

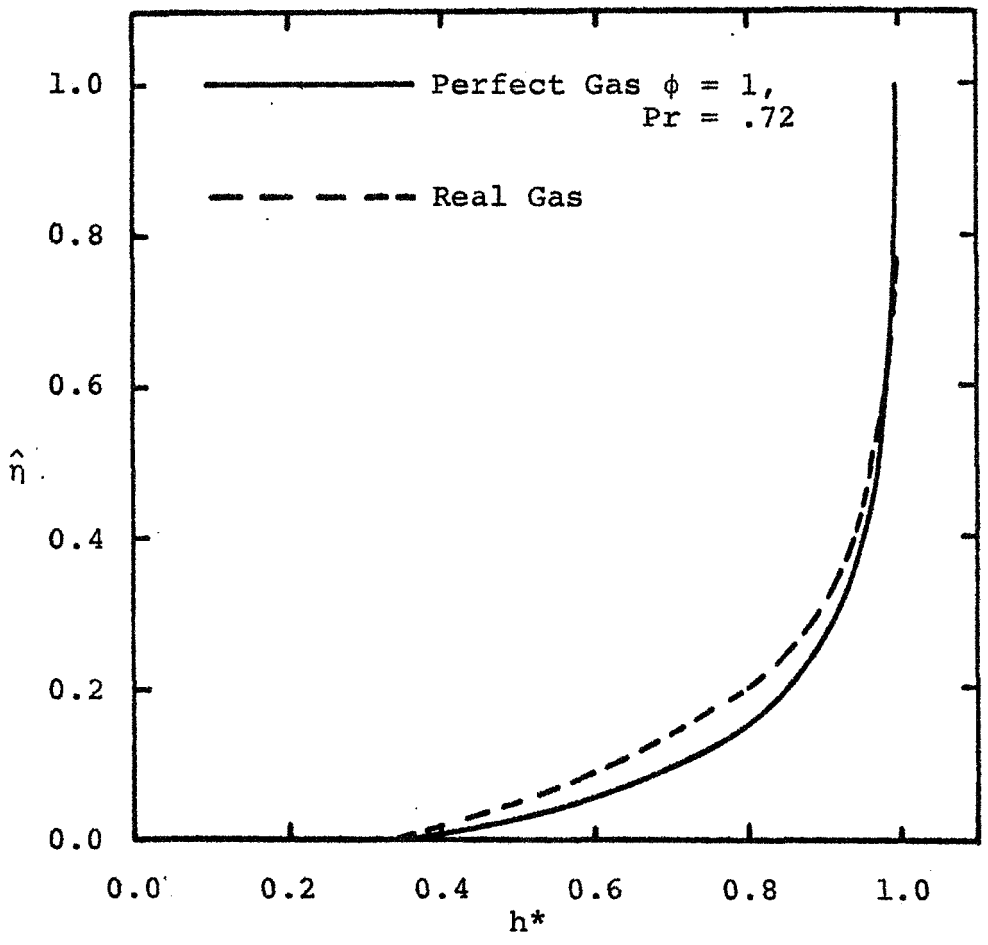

Figure 11a. Comparison of Enthalpy Profile at $\hat{\xi} = 0.1$ for Real and Perfect Gas Solutions, w = 4, Second Approximation.

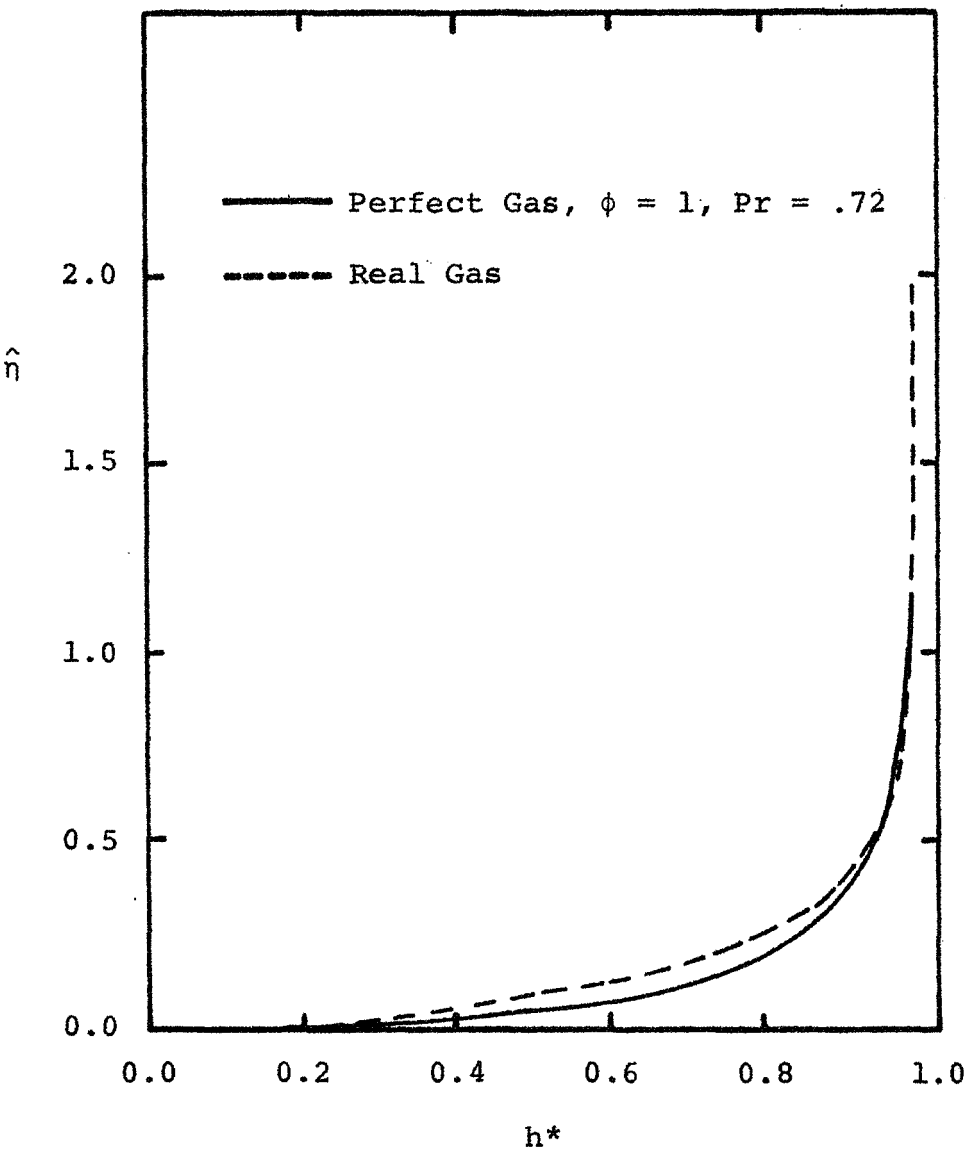

Figure 11b. Comparison of Enthalpy Profiles at $\hat{\xi}$ = .21 for Real and Perfect Gas Solutions, w = 5, Second Approximation.

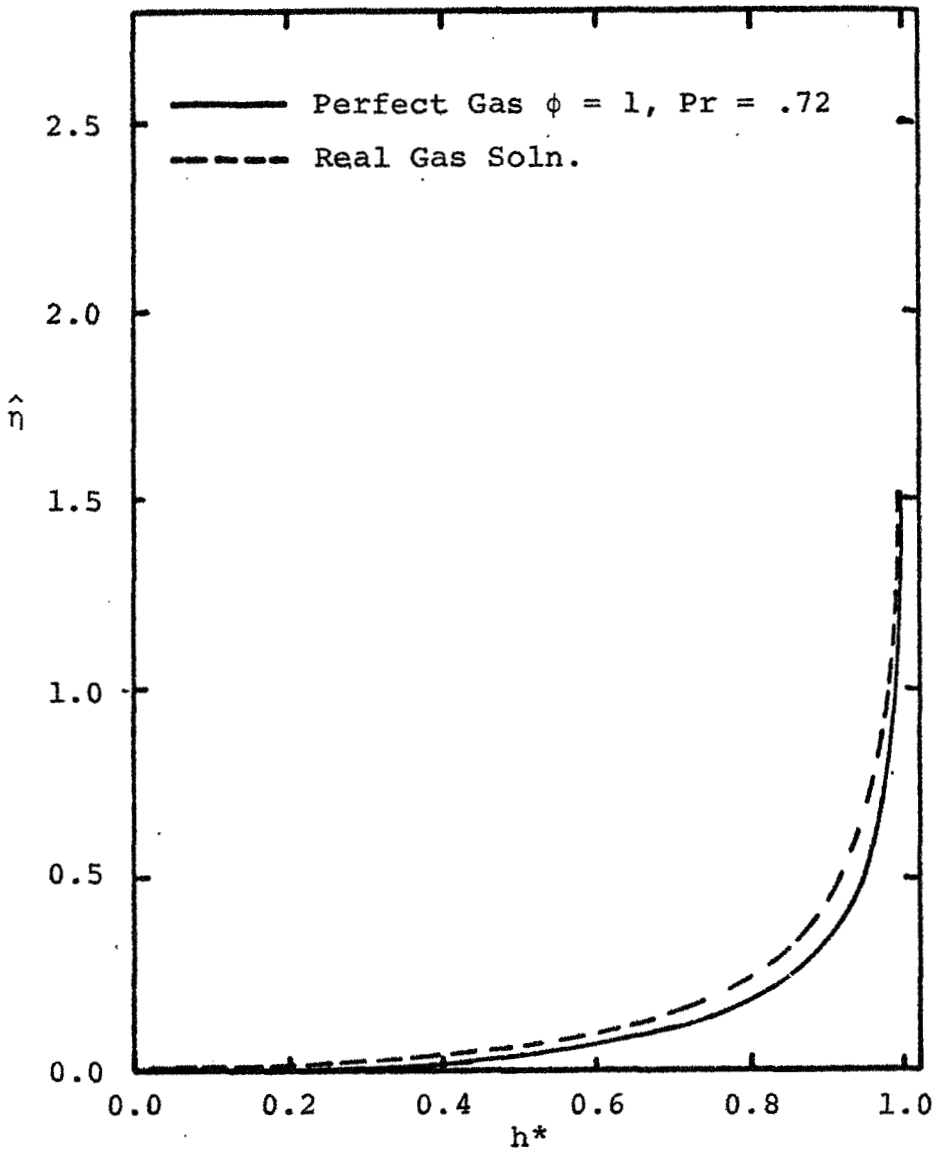

Figure 11c. Comparison of Enthalpy Profile at $\hat{\xi}$ = .25 for Real and Perfect Gas Solutions, w = 6, Second Approximation.

6. SUMMARY AND CONCLUSIONS

The laminar boundary layer immediately behind a shock wave moving over a flat plate has been analyzed for both a perfect gas and a real gas in thermodynamic equilibrium. The method of weighted residuals was employed as an approximation technique for solving the appropriate partial differential equations and the results for a perfect gas were compared with those of Mirels [1], and where applicable, the solution given by Lam and Crocco [4].

It was found that, for a perfect gas, the first MWR approximation led to a simple analytical solution which agreed remarkably well with the more accurate solutions of Mirels. Further, it was shown that higher MWR solutions could theoretically be obtained from simple algebraic equations (for a perfect gas) to any desired accuracy.

By reverting to a shock-fixed coordinate system an MWR second approximation numerical solution was obtained for both a perfect and a real gas (nitrogen). This led to very accurate boundary-layer parameter calculations when compared with Mirels' [1] perfect gas results. It was also possible to compare the effects of real gas behavior on the boundary layer and, as expected indicated increasing departure from perfect gas computations as the shock strength increases.

The primary utility of the work reported herein is its application to the shock induced flow over a semi-infinite flat plate where the leading-edge effect is taken into account. This extension, where boundary-layer assumptions are retained, is given in a companion report.

7. REFERENCES

1. Mirels, H.: Boundary Layer Behind Shock or Thin Expansion Wave Moving Into Stationary Fluid. NACA TN-3712. May, 1956.

2. Ackroyd, J. A. D.: On the Laminar Compressible Boundary Layer Induced by the Passage of Plane Shock Wave Over a Flat Wall. A.R.C. 28-456 Hyp. 586, 1966.

3. Ackroyd, J. A. D.: Some further Notes on the Laminar Boundary Layer Development and Running Time in a Shock Tube. A.R.C. C.P. No. 966, 1967.

4. Lam, S. H., and Crocco, L.: "Shock Induced Unsteady Laminar Compressible Boundary Layer On a Semi-Infinite Flat Plate". Princeton University Report No. 428 AFOSR TN 58-581, AD 162-101, Sept., 1958.

5. Hall, M. G.: "The Boundary Layer Over an Impulsively-Started Plate", Technical Report 68088, Royal Aircraft Establishment, April, 1968.

6. Hall, M. G.: "The Boundary Layer Over an Impulsively-Started Flat Plate", Proc. Roy. Soc., A, Vol. 310, 1969.

7. Hall, M. G.: "A Numerical Method for Calculating Unsteady Two-Dimensional Laminar Boundary Layers", Ingenieur Archiv, 38 Band, 1969.

8. Abbott, D. E. and Bethel, H. E.: Application of the Galerkin-Kantorovich-Dorodnitsyn Method of Integral Relations to the Solution of Steady Laminar Boundary Layers. Ingenieur-Archiv, 37 Band, 2 Heft, 1968.

9. Abbott, D. E., Deiwert, G. S., Forsnes, V. G. and Deboy, G. R.: The Method of Weighted Residuals as a Solution Technique. Proceedings, Computation of Turbulent Boundary Layers, Vol. I, Stanford University, 1968.

10. Deiwert, G. S. and Abbott, D. E.: Analytical Prediction of the Incompressible Turbulent Boundary Layer with Arbitrary Pressure Distribution. AIAA, Journal of Hydronautics, Vol. 4, No. 1, January 1970, pp. 27-34.

11. Koob, S. J. and Abbott, D. E.: Investigation of a Method for the General Analysis of Time Dependent Two-Dimensional Laminar Boundary Layers. J. of Basic Engineering, December, 1968.

12. Goodwin, F. K., Nielsen, J. N., and Lynes, L. L.: Recent Applications of the Method of Integral Relations to Laminar Boundary Layer Problems. AIAA Paper No. 68-738, AIAA Fluid and Plasma Dynamics Conference, Los Angeles, California, 1968.

13. Pavlovskii, Y. N.: Numerical Solution of the Boundary Layer in a Compressible Gas. (Translation from the Journ. of Comp. Math. and Mathematical Phys., Aca. of Sci. USSR., Vol. 2, No. 5, Sept-Oct., 1962. Translated by Strelhoff, edited by M. Holt under AFOSR 268-63.

14. Ahtye, W. F., and Peng, Tzy-Cheng: Approximations for Thermodynamic and Transport Properties of High Temperature Nitrogen with Shock-Tube Applications. NASA-TN D-1303, 1962.

15. Marvin, J. G., and Deiwert, G. S.: Convective Heat Transfer in Planetary Gases. NASA TR R-224. July, 1965.

Table 1a

Boundary-layer Parameters for w = 2, Perfect Gas Solution, $\phi = 1$, Pr = .72

Second Approximation

$\hat{\xi}$	$-\rho_0\hat{\theta}_0$	$\hat{C}_f\sqrt{\hat{Re}_L}$	$\frac{\delta}{L}\sqrt{\hat{Re}_L}$	$\frac{\delta^*}{\delta}$	$\frac{\delta^{**}}{\delta}$	$\frac{\delta^{***}}{\delta}$	$\frac{Nu(1-h_0)}{\hat{Re}_L^{0.5}}$
0.05	0.31148	3.21053	0.98035	0.20680	0.32872	0.61526	1.36944
0.10	0.44051	2.27011	1.37178	0.20798	0.33085	0.62513	0.96831
0.15	0.53952	1.85351	1.68010	0.20798	0.33085	0.62513	0.79061
0.20	0.62298	1.60518	1.94003	0.20798	0.33085	0.62513	0.68469
0.25	0.69652	1.43571	2.16902	0.20798	0.33085	0.62513	0.61240
0.30	0.76300	1.31062	2.37605	0.20798	0.33085	0.62513	0.55904
0.35	0.82413	1.21339	2.56643	0.20798	0.33085	0.62513	0.51757
0.40	0.88104	1.13503	2.74364	0.20798	0.33085	0.62514	0.48414
0.45	0.93448	1.07011	2.91007	0.20798	0.33085	0.62513	0.45645
0.50	0.98503	1.01520	3.06748	0.20798	0.33085	0.62514	0.43303
0.55	1.03311	0.96795	3.21721	0.20798	0.33085	0.62513	0.41288
0.60	1.07905	0.92674	3.36027	0.20798	0.33085	0.62513	0.39530
0.65	1.12311	0.89038	3.49321	0.20811	0.33110	0.62627	0.37979
0.70	1.16551	0.85799	3.62950	0.20798	0.33085	0.62514	0.36598
0.75	1.20642	0.82890	3.75690	0.20798	0.33085	0.62513	0.35357
0.80	1.24598	0.80258	3.88011	0.20798	0.33085	0.62513	0.34234
0.85	1.28433	0.77862	3.99952	0.20798	0.33085	0.62514	0.33212
0.90	1.32156	0.75668	4.11547	0.20798	0.33085	0.62513	0.32276
0.95	1.35778	0.73650	4.22825	0.20798	0.33085	0.62514	0.31415
1.00	1.39305	0.71785	4.53101	0.20324	0.32226	0.58547	0.30620

Table 1b

Boundary-layer Parameters for w = 4, Perfect Gas Solution, $\phi = 1$, Pr = .72

Second Approximation

$\hat{\xi}$	$-\rho_0\hat{\theta}_0$	$-\hat{C}_f\sqrt{\hat{Re}_L}$	$\frac{\delta}{L}\sqrt{\hat{Re}_L}$	$\frac{\delta^*}{\delta}$	$\frac{\delta^{**}}{\delta}$	$\frac{\delta^{***}}{\delta}$	$\frac{Nu(1-h_0)}{\hat{Re}_L^{0.5}}$
0.05	0.07950	12.57898	1.12008	0.14193	0.39034	0.56780	10.39090
0.10	0.11012	9.08130	1.54227	0.14277	0.39267	0.57119	7.39776
0.15	0.13490	7.41296	1.90618	0.14152	0.38921	0.56616	6.16506
0.20	0.15578	6.41944	2.19480	0.14193	0.39034	0.56780	5.30280
0.25	0.17425	5.73897	2.45504	0.14193	0.39034	0.56780	4.74069
0.30	0.19102	5.23492	2.69148	0.14192	0.39033	0.56779	4.32451
0.35	0.20629	4.84759	2.90649	0.14193	0.39034	0.56780	4.00441
0.40	0.22038	4.53763	3.10364	0.14199	0.39051	0.56805	3.74444
0.45	0.23032	4.34186	3.24417	0.14196	0.39044	0.56795	3.58443
0.50	0.24646	4.05737	3.47273	0.14192	0.39032	0.56777	3.35201
0.55	0.25847	3.86886	3.64202	0.14192	0.39031	0.56776	3.19645
0.60	0.26994	3.70457	3.80330	0.14193	0.39034	0.56780	3.06026
0.65	0.28095	3.55929	3.95924	0.14192	0.39030	0.56782	2.94016
0.70	0.29155	3.42989	4.10871	0.14192	0.39030	0.56782	2.83327
0.75	0.30178	3.31371	4.25005	0.14195	0.39042	0.56777	2.73730
0.80	0.31166	3.20858	4.38253	0.14201	0.39072	0.56766	2.65046
0.85	0.32124	3.11294	4.51179	0.14207	0.39095	0.56758	2.57145
0.90	0.33054	3.02534	4.64508	0.14204	0.39084	0.56762	2.49909
0.95	0.33959	2.94476	4.77906	0.14198	0.39056	0.56772	2.43252
1.00	0.34840	2.87028	4.90918	0.14192	0.39032	0.56781	2.37100

Table 1c

Boundary-layer Parameters for w = 6, Perfect Gas Solution, $\phi = 1$, Pr = .72

Second Approximation

$\hat{\xi}$	$-\rho_0\hat{\theta}_0$	$-\hat{C}_f\sqrt{\hat{Re}_L}$	$\frac{\delta}{L}\sqrt{\hat{Re}_L}$	$\frac{\delta^*}{\delta}$	$\frac{\delta^{**}}{\delta}$	$\frac{\delta^{***}}{\delta}$
0.05	0.04050	24.68906	1.23233	0.11090	0.43269	1.39185
0.10	0.05513	18.14000	1.67723	0.11090	0.43269	1.39185
0.15	0.06751	14.81155	2.05414	0.11090	0.43269	1.39185
0.20	0.07796	12.82734	2.37188	0.11090	0.43269	1.39185
0.25	0.08716	11.47295	2.65189	0.11090	0.43269	1.39185
0.30	0.09548	10.47342	2.90490	0.11090	0.43270	1.39185
0.35	0.10313	9.69659	3.13766	0.11090	0.43269	1.39185
0.40	0.11025	9.07038	3.35432	0.11090	0.43269	1.39185
0.45	0.11694	8.55158	3.55784	0.11090	0.43269	1.39184
0.50	0.12326	8.11272	3.75031	0.11090	0.43269	1.39184
0.55	0.12928	7.73521	3.93330	0.11090	0.43269	1.39185
0.60	0.13503	7.40592	4.10819	0.11090	0.43269	1.39185
0.65	0.14055	7.11513	4.27609	0.11090	0.43269	1.39185
0.70	0.14586	6.85603	4.43770	0.11090	0.43269	1.39185
0.75	0.15098	6.62340	4.59356	0.11090	0.43269	1.39185
0.80	0.15593	6.41297	4.74428	0.11090	0.43269	1.39185
0.85	0.16073	6.22156	4.89025	0.11090	0.43269	1.39185
0.90	0.16539	6.04628	5.03201	0.11090	0.43269	1.39185
0.95	0.16992	5.88503	5.16989	0.11090	0.43269	1.39185
1.00	0.17434	5.73606	5.30416	0.11090	0.43269	1.39185

Table 2a

Velocity Profile Dependence on Distance from Fixed Shock

$w = 2,\ \phi = 1,\ Pr = .72$

Second Approximation

u**	$\frac{Y}{L}\sqrt{\hat{Re}_L}$				
	$\xi=.1$	$\xi=.3$	$\xi=.5$	$\xi=.7$	$\xi=.9$
2.000	0.CCC00	0.0CC00	0.00000	0.00000	0.00000
1.800	0.06819	0.11812	0.15249	0.18043	0.20459
1.600	0.14787	C.25613	0.33067	0.39125	0.44364
1.500	0.19456	0.33700	0.43507	0.51478	0.58371
1.400	0.24852	0.43046	0.55572	0.65754	0.74558
1.300	0.31396	0.54381	0.70206	0.83069	0.94192
1.200	0.40037	C.69348	0.89528	1.05931	1.20115
1.100	0.53799	0.93184	1.20301	1.42342	1.61401
1.010	0.96065	1.66393	2.14814	2.54171	2.88203
1.001	1.37178	2.37605	3.06748	3.62950	4.11547

Table 2b

Velocity Profile Dependence on Distance from Fixed Shock

$w = 4$, $\phi = 1$, $Pr = .72$

Second Approximation

u**	$\frac{Y}{L}\sqrt{\hat{Re}_L}$				
	$\hat{\xi}=.1$	$\hat{\xi}=.3$	$\hat{\xi}=.5$	$\hat{\xi}=.7$	$\hat{\xi}=.9$
4.000	0.00000	0.00000	0.00000	0.00000	0.00000
3.750	0.01032	0.01792	0.02312	0.02735	0.03100
3.500	0.02234	0.03879	0.05005	0.05921	0.06709
3.250	0.03640	0.06324	0.08159	0.09652	0.10935
3.000	0.05300	0.09210	0.11883	0.14058	0.15924
2.750	0.07280	0.12657	0.16330	0.19319	0.21879
2.500	0.09680	0.16837	0.21723	0.25699	0.29100
2.250	0.12654	0.22019	0.28409	0.33609	0.38049
2.000	0.16460	0.28653	0.36969	0.43736	0.49504
1.800	0.20414	0.35547	0.45865	0.54261	0.61407
1.600	0.25682	0.44737	0.57722	0.68290	0.77271
1.500	0.29100	0.50701	0.65417	0.77394	0.87565
1.400	0.33350	0.58117	0.74986	0.88715	1.00364
1.300	0.38915	0.67828	0.87516	1.03540	1.17124
1.200	0.46879	0.81729	1.05452	1.24760	1.41113
1.100	0.60703	1.05862	1.36590	1.61602	1.82758
1.010	1.07345	1.87294	2.41659	2.85914	3.23270
1.001	1.54227	2.69148	3.47273	4.10871	4.64508

Table 2c

Velocity Profile Dependence on Distance from Fixed Shock

$w = 6,\ \phi = 1,\ Pr = .72$

Second Approximation

	$\frac{y}{L}\sqrt{\hat{Re}_L}$				
u**	$\hat{\xi}$=.1	$\hat{\xi}$=.3	$\hat{\xi}$=.5	$\hat{\xi}$=.7	$\hat{\xi}$=.9
6.000	0.00000	0.00000	0.00000	0.00000	0.00000
5.750	0.00029	0.00050	0.00065	0.00076	0.00087
5.500	0.00120	0.00207	0.00267	0.00317	0.00359
5.250	0.00279	0.00484	0.00625	0.00739	0.00838
5.000	0.00516	0.00894	0.01155	0.01366	0.01549
4.750	0.00841	0.01456	0.01880	0.02225	0.02523
4.500	0.01265	0.02190	0.02828	0.03346	0.03794
4.250	0.01802	0.03122	0.04030	0.04769	0.05408
4.000	0.02473	0.04283	0.05529	0.06543	0.07419
3.750	0.03299	0.05713	0.07376	0.08727	0.09896
3.500	0.04309	0.07464	0.09636	0.11402	0.12929
3.250	0.05545	0.09603	0.12398	0.14670	0.16635
3.000	0.07057	0.12222	0.15780	0.18672	0.21172
2.750	0.08921	0.15450	0.19947	0.23603	0.26764
2.500	0.11244	0.19475	0.25143	0.29751	0.33736
2.250	0.14197	0.24588	0.31744	0.37562	0.42593
2.000	0.18060	0.31279	0.40382	0.47783	0.54183
1.800	0.22146	0.38356	0.49519	0.58595	0.66442
1.600	0.27672	0.47927	0.61875	0.73216	0.83022
1.500	0.31294	0.54200	0.69973	0.82798	0.93887
1.400	0.35826	0.62049	0.80108	0.94790	1.07485
1.300	0.41798	0.72393	0.93462	1.10592	1.25403
1.200	0.50399	0.87289	1.12692	1.33347	1.51206
1.100	0.65417	1.13301	1.46274	1.73084	1.96265
1.010	1.16389	2.01582	2.60249	3.07949	3.49190
1.001	1.67723	2.90490	3.75031	4.43770	5.03201

Table 3a

Boundary-layer Parameters for w = 2, Real Gas Solution; Nitrogen

Second Approximation

$\hat{\xi}$	$-\rho_0\hat{\theta}_0$	$-C_f\sqrt{\hat{Re}_L}$	$\frac{\delta}{L}\sqrt{\hat{Re}_L}$	$\frac{\delta^*}{\delta}$	$\frac{\delta^{**}}{\delta}$	$\frac{\delta^{***}}{\delta}$	$\frac{Nu(1-h_0)}{\hat{Re}_L^{0.5}}$
0.05	0.31148	3.39285	1.18383	0.17041	0.27108	0.51220	2.95278
0.10	0.44051	2.39903	1.68529	0.16929	0.26931	0.50884	2.12876
0.15	0.53952	1.95878	2.07122	0.16870	0.26838	0.50709	1.75573
0.20	0.62298	1.69634	2.39714	0.16832	0.26776	0.50593	1.53066
0.25	0.69652	1.51725	2.68463	0.16803	0.26731	0.50507	1.37578
0.30	0.76300	1.38505	2.94478	0.16781	0.26696	0.50440	1.26073
0.35	0.82413	1.28231	3.18419	0.16763	0.26667	0.50385	1.17087
0.40	0.88104	1.19949	3.40717	0.16747	0.26642	0.50339	1.09813
0.45	0.93448	1.13088	3.61671	0.16734	0.26621	0.50300	1.03768
0.50	0.98503	1.07285	3.81498	0.16723	0.26603	0.50265	0.98637
0.55	1.03255	1.02348	4.00563	0.16704	0.26571	0.50153	0.94263
0.60	1.07905	0.97937	4.18397	0.16703	0.26572	0.50206	0.90343
0.65	1.12880	0.93621	4.37931	0.16694	0.26557	0.50178	0.86500
0.70	1.16551	0.90672	4.52351	0.16687	0.26547	0.50159	0.83869
0.75	1.20641	0.87598	4.68420	0.16680	0.26535	0.50138	0.81122
0.80	1.24599	0.84815	4.83977	0.16674	0.26525	0.50118	0.78631
0.85	1.28433	0.82284	4.99045	0.16668	0.26516	0.50101	0.76362
0.90	1.26812	0.83335	5.32445	0.16069	0.25398	0.44325	0.77410
0.95	1.36902	0.77193	5.32348	0.16656	0.26496	0.50063	0.71789
1.00	1.39603	0.75700	5.42969	0.16652	0.26490	0.50052	0.70445

Table 3b

Boundary-layer Parameters for w = 4, Real Gas Solution; Nitrogen

Second Approximation

$\hat{\xi}$	$-\rho_0\hat{\theta}_0$	$-\hat{C}_f\sqrt{\hat{Re}_L}$	$\frac{\delta}{L}\sqrt{\hat{Re}_L}$	$\frac{\delta^*}{\delta}$	$\frac{\delta^{**}}{\delta}$	$\frac{\delta^{***}}{\delta}$	$\frac{Nu(1-h_0)}{\hat{Re}_L^{0.5}}$
0.05	0.07784	17.42214	0.86509	0.17994	0.49488	0.71988	5.38205
0.10	0.11009	12.31886	1.22347	0.17994	0.49488	0.71987	3.80565
0.15	0.13484	10.05817	1.49846	0.17994	0.49488	0.71987	3.10728
0.20	0.15570	8.71055	1.73029	0.17994	0.49488	0.71987	2.69097
0.25	0.17408	7.79093	1.93453	0.17994	0.49488	0.71987	2.40687
0.30	0.19069	7.11210	2.11918	0.17994	0.49488	0.71987	2.19716
0.35	0.20597	6.58451	2.28898	0.17994	0.49488	0.71987	2.03417
0.40	0.22019	6.15924	2.44702	0.17994	0.49488	0.71987	1.90279
0.45	0.23355	5.80698	2.59546	0.17994	0.49488	0.71987	1.79397
0.50	0.24618	5.50898	2.73586	0.17994	0.49488	0.71987	1.70191
0.55	0.25820	5.25261	2.86939	0.17994	0.49488	0.71987	1.62271
0.60	0.26968	5.02899	2.99699	0.17994	0.49488	0.71987	1.55362
0.65	0.28069	4.83169	3.11936	0.17994	0.49488	0.71987	1.49267
0.70	0.29129	4.65594	3.23712	0.17994	0.49488	0.71987	1.43838
0.75	0.30151	4.49806	3.35074	0.17994	0.49488	0.71987	1.38960
0.80	0.31140	4.35522	3.46063	0.17994	0.49488	0.71987	1.34548
0.85	0.32098	4.22519	3.56714	0.17994	0.49488	0.71987	1.30530
0.90	0.33029	4.10614	3.67055	0.17994	0.49488	0.71987	1.26853
0.95	0.33934	3.99663	3.77113	0.17994	0.49488	0.71987	1.23469
1.00	0.34816	3.89543	3.86910	0.17994	0.49488	0.71987	1.20343

Table 3c

Boundary-layer Parameters for w = 6, Real Gas Solution; Nitrogen

Second Approximation

$\hat{\xi}$	$-\rho_0\hat{\theta}_0$	$-\hat{C}_f\sqrt{Re_L}$	$\frac{\delta}{L}\sqrt{\hat{Re}_L}$	$\frac{\delta^*}{\delta}$	$\frac{\delta^{**}}{\delta}$	$\frac{\delta^{***}}{\delta}$
0.05	0.03878	122.98341	1.11012	0.11779	0.45968	1.47850
0.10	0.10823	44.06231	1.57573	0.11785	0.60041	1.63633
0.15	0.28763	16.57948	1.91855	0.11798	0.93910	2.01616
0.20	0.07755	61.49108	2.22039	0.11779	0.45967	1.47849
0.25	0.08666	55.02663	2.47688	0.11779	0.45992	1.47878
0.30	0.09494	50.23018	2.71695	0.11779	0.45973	1.47856
0.35	0.10260	46.47796	2.93903	0.11779	0.45960	1.47841
0.40	0.10969	43.47316	3.14302	0.11779	0.45956	1.47837
0.45	0.11619	41.04356	3.33172	0.11779	0.45944	1.47824
0.50	0.12229	38.99511	3.50898	0.11779	0.45935	1.47813
0.55	0.12833	37.15943	3.68091	0.11779	0.45941	1.47820
0.60	0.13423	35.52731	3.84691	0.11779	0.45952	1.47833
0.65	0.13988	34.09157	4.00632	0.11779	0.45962	1.47843
0.70	0.14524	32.83408	4.15936	0.11779	0.45963	1.47845
0.75	0.15037	31.71259	4.30650	0.11779	0.45963	1.47845
0.80	0.15534	30.69803	4.44774	0.11779	0.45966	1.47849
0.85	0.16016	29.77395	4.58362	0.11779	0.45973	1.47856
0.90	0.16484	28.93022	4.71493	0.11779	0.45981	1.47865
0.95	0.16937	28.15616	4.84228	0.11779	0.45988	1.47872
1.00	0.17377	27.44274	4.96629	0.11779	0.45993	1.47878

APPENDICES

APPENDIX A

ON THE DETERMINATION OF COEFFICIENTS IN APPROXIMATING FUNCTIONS

In this appendix, a procedure is given for computing the coefficients in the approximation functions. The variables whose coefficients are required are $\rho^*\theta$, h^*, ϕ, ϕ/Pr, and the physical conditions which must be preserved by the functional approximations have been given in detail in Section 3.1. The equations for determining the N coefficients in the approximation function for an arbitrary variable $\psi(u^*)$, is obtained by collocation:

$$\psi(u^*) = \sum_{i=0}^{N-1} a_i u^{*i} \tag{A.1}$$

where it is recalled, N=1, 2 . . . correspond to the order of approximation in this study, and $0 \leq u^* \leq 1$. Any method may be adopted for choosing values of u^* in the allowable interval for which equation A.1 is exact. A compatible system of simultaneous equations is obtained in the form stated below if exactly N collocation points are taken;

$$\begin{bmatrix} 1 & u_0^* & u_0^{*2} & \cdots & u_0^{*N-1} \\ 1 & u_1^* & u_1^{*2} & \cdots & u_1^{*N-1} \\ \cdot & \cdot & \cdot & \cdots & \cdot \\ \cdot & \cdot & \cdot & \cdots & \cdot \\ 1 & u_{N-2}^* & u_{N-2}^{*2} & \cdots & u_{N-2}^{*N-1} \\ 1 & u_{N-1}^* & u_{N-1}^{*2} & \cdots & u_{N-2}^{*N-1} \end{bmatrix} \begin{bmatrix} a_0 \\ a_1 \\ \cdot \\ \cdot \\ a_{N-2} \\ a_{N-1} \end{bmatrix} = \begin{bmatrix} \psi_0 \\ \psi_1 \\ \cdot \\ \cdot \\ \psi_{N-2} \\ \psi_{N-1} \end{bmatrix} \tag{A.2}$$

or the redundant system below

$$\begin{bmatrix} 1 & u_0^* & u_0^{*2} & \cdots & u_0^{*N-1} \\ 1 & u_1^* & u_1^{*2} & \cdots & u_1^{*N-1} \\ \cdot & & & \cdots & \\ \cdot & \cdot & \cdot & \cdots & \\ 1 & u_{N-2}^* & u_{N-2}^{*2} & \cdots & u_{N-2}^{*N-1} \\ 1 & u_{N-1}^* & u_{N-2}^{*2} & \cdots & u_{N-1}^{*N-1} \\ 1 & u_N^* & u_N^{*2} & \cdots & u_N^{*N-1} \\ \cdot & & & \cdots & \\ \cdot & \cdot & \cdot & \cdots & \\ 1 & u_{N+j-1}^* & u_{N+j-1}^{*2} & \cdots & u_{N+j-1}^{*N-1} \end{bmatrix} \begin{bmatrix} a_0 \\ a_1 \\ \cdot \\ \cdot \\ a_{N-2} \\ a_{N-1} \\ \\ \\ \\ \end{bmatrix} = \begin{bmatrix} \psi_0 \\ \psi_1 \\ \cdot \\ \cdot \\ \psi_{N-2} \\ \psi_{N-1} \\ \psi_N \\ \cdot \\ \cdot \\ \psi_{N+j-1} \end{bmatrix} \qquad (A.3)$$

if more collocation points than the minimum required to solve for a_i in equation (A.1) are taken. It is clear that equations (A.2) and (A.3) are identical for j=0. The system in equation (A.2) can be solved easily and exactly for small values of N. For higher values of N, and in general, equation (A.3) must be solved by any approximate methods; least-square or regression methods are recommended.

In this study, the points for collocation are chosen such that

$$u_i^* = \frac{i}{N} \qquad (A.4)$$

where i = 0, 1, 2, . . N-1

and

$$\psi_i = \psi(u_i^* = i/N) \tag{A.5}$$

where i = 0, 1, 2, . . N-1

A.1 Approximating Functions in Plate-Fixed Coordinate System

In the plate fixed reference, equation (A.4) gives the points of collocation.

In the scheme of the first order approximation, and the collocation procedure defined above, the following equations are obtained,

$$\rho^*\theta \cong \frac{\rho_0\theta_0}{1-u^*} \tag{A.6}$$

$$\frac{1}{\rho^*\theta} \cong \frac{1-u^*}{\rho_0\theta_0} \tag{A.7}$$

$$\psi \cong \psi_0 + (1-\psi_0)\, u^* \tag{A.8}$$

and in the scheme of the second order approximation;

$$\rho^*\theta \cong \frac{1}{1-u^*}\left[(1-2u^*)\,\rho_0\theta_0 + u^*\rho_1\theta_1\right] \tag{A.9}$$

$$\frac{Q}{\rho^*\theta} \cong (1-u^*)\left[(1-2u^*)\,\frac{Q_0}{\rho_0\theta_0} + 4u^*\frac{Q_1}{\rho_1\theta_1}\right] \tag{A.10}$$

$$\psi \cong \psi_0 + (-3\psi_0 + 4\psi_1 - 1)u^* + (2\psi_0 - 4\psi_1 + 2)u^{*2} \tag{A.11a}$$

where

$$\psi \equiv \begin{cases} \rho^* \\ h^* \\ \phi \\ \dfrac{\phi}{Pr} \end{cases} \qquad \text{(A.11b)}$$

A.2 Approximating Functions in Shock-fixed Coordinate System

The collocation procedure in this reference system is the same as defined above, except the choice of collocation points need to be modified. Because the velocity at the wall is finite in this case, the corresponding collocation points are obtained at

$$u_i^{**} = w + (1-w)\frac{i}{N} \qquad \text{(A.12)}$$

where $i = 0, 1, 2, \ldots N-1$

When w is replaced by zero in equation (A.12), a direct algebraic correspondence can be seen between this equation and equation (A.4). With the variable which is to be approximated given by

$$\psi_i = \psi(u^{**} = u_i^{**}) \qquad \text{(A.13)}$$

Equation (A.1) can be used for calculating the coefficients a_i.

The approximation functions under the first order approximation are obtained by setting N equal to unity in the collocation equation (A.1), and using equations (A.12) and (A.13) to choose the collocation points yields:

$$\rho^*\hat{\theta} \cong \frac{1-w}{1-u^{**}}\ \rho_0\hat{\theta}_0 \tag{A.14}$$

$$\frac{Q}{\rho^*\hat{\theta}} \cong \frac{1-u^{**}}{1-w}\ \frac{Q_0}{\rho_0\hat{\theta}_0} \tag{A.15}$$

$$\psi \cong \frac{1}{1-w}\ [\psi_0 - w + (1-\psi_0)\ u^{**}] \tag{A.16}$$

In equation (A.16), the identities given by equation (A.11b) are assumed.

In the second order approximation, N is set equal to two in equation (A.1), and the collocation points are chosen as in the section above; this leads to the following equations:

$$\rho^*\hat{\theta} \cong \frac{1}{1-u^{**}}\ [(w+1-2u^{**})\rho_0\hat{\theta}_0 + (u^{**}-w)\rho_1\hat{\theta}_1] \tag{A.17}$$

$$\frac{Q}{\rho^*\hat{\theta}} \cong \frac{1-u^{**}}{(1-w)^2}\ [(w+1-2u^{**})\rho_0\hat{\theta}_0 + 4(u^{**}-w)\rho_1\hat{\theta}_1] \tag{A.18}$$

and

$$\begin{aligned}\psi = {} & a_{11}\psi_0 + a_{21}\psi_1 + a_{31} \\ & + (a_{12}\psi_0 + a_{22}\psi_1 + a_{33})u^{**} \\ & + (a_{13}\psi_0 + a_{23}\psi_1 + a_{33})u^{**2}\end{aligned} \tag{A.19}$$

where

$$a_{11} = \frac{w+1}{(1-w)^2}$$

$$a_{12} = -\frac{w+3}{(1-w)^2}$$

$$a_{13} = \frac{2}{(1-w)^2} \qquad \text{(A.20)}$$

$$a_{21} = -\frac{4w}{(1-w)^2}$$

$$a_{22} = \frac{4(w+1)}{(1-w)^2}$$

$$a_{23} = -\frac{4}{(1-w)^2} \qquad \text{(A.21)}$$

$$a_{31} = \frac{w(w+1)}{(1-w)^2}$$

$$a_{32} = -\frac{1+3w}{(1-w)^2}$$

$$a_{33} = \frac{2}{(1-w)^2} \qquad \text{(A.22)}$$

The procedure outlined above can be routinely extended to higher values of N. It may be pointed out that in the above equations, the equality sign has been used where it is strictly correct in the mathematical sense. The approximation functions are exact only at the collocation points and errors are expected at intermediate points.

APPENDIX B

DERIVATION OF ENERGY DIFFERENTIAL EQUATION FOR SHOCK-FIXED ANALYSIS

The steps for reducing equation (5.14) to the form given by equation (5.22) was omitted. In this appendix the functional relations defining RHS, LHS and AH in equation (5.22) will be derived.

With the aid of a weighting function given by

$$f_i(u^{**}) = (1-u^{**})^i \tag{5.22}$$

and approximating functions defined in A.2, the integro-differential equation

$$\begin{aligned}\frac{\partial}{\partial\hat{\xi}}\int_w^1 f_i(u^{**})h^*\rho^*\theta u^{**}du^{**} &= -\left[f_i(u^{**})\frac{\partial h^*}{\partial u^{**}}\frac{\phi}{Pr}\frac{1}{\rho^*\hat{\theta}}\right]_{u^{**}=w} \\ &-\left[f_i'(u^{**})h^*\frac{\phi}{\rho^*\hat{\theta}}\right]_{u^{**}=w} - \int_w^1\left(\phi+\frac{\phi}{Pr}\right)\frac{\partial h^*}{\partial u^{**}}\frac{f_i(u^{**})}{\rho^*\hat{\theta}}du^{**} \\ &-\int_w^1 h^*f_i''(u^{**})\frac{\phi}{\rho^*\hat{\theta}}du^{**} + \frac{\hat{U}_e^2}{g_c J h_e}\int_w^1\frac{\phi}{\rho^*\hat{\theta}}f_i(u^{**})\,du^{**}\end{aligned} \tag{5.14}$$

can be integrated analytically. It is convenient to define the following functional groups

$$LA = \frac{\partial}{\partial \hat{\xi}} \int_w^1 f_i(u^{**}) h^* \rho^* \hat{\theta} u^{**} du^{**} \tag{B.1}$$

$$RA = -\left[f_i(u^{**}) \frac{\partial h^*}{\partial u^{**}} \frac{\phi}{Pr} \frac{1}{\rho^* \hat{\theta}} \right]_{u^{**}=w} - \left[f_i'(u^{**}) h^* \frac{\phi}{\rho^* \hat{\theta}} \right]_{u^{**}=w} \tag{B.2}$$

$$RB = -\int_w^1 \left(\phi + \frac{\phi}{Pr} \right) \frac{\partial h^*}{\partial u^{**}} \frac{f_i(u^{**})}{\rho^* \hat{\theta}} du^{**} \tag{B.3}$$

$$RC = -\int_w^1 h^* f_i''(u^{**}) \frac{\phi}{\rho^* \hat{\theta}} du^{**} \tag{B.4}$$

$$RD = \frac{\hat{U}_e^2}{g_c J h_e} \int_w^1 \frac{\phi}{\rho^* \hat{\theta}} f_i(u^{**}) du^{**} \tag{B.5}$$

Substituting the approximating functions obtained in Appendix A.2 for h^*, $\rho^* \hat{\theta}$ and $Q/\rho^* \hat{\theta}$ the following results are obtained:

$$\begin{aligned} LA = \frac{\partial}{\partial \hat{\xi}} [& AB(w,h_0,h_1)\ AB1(w,\rho_0\hat{\theta}_0,\rho_1\hat{\theta}_1) \\ & + AC(w,h_0,h_1)\ AC1(w,\rho_0\hat{\theta}_0,\rho_1\hat{\theta}_1) \\ & + AD(w,h_0,h_1)\ AD1(w,\rho_0\hat{\theta}_0,\rho_1\hat{\theta}_1)] \end{aligned} \tag{B.6}$$

where

$$AB(w,h_0,h_1) = \frac{1}{(1-w)^2} [(w+1)h_0 - 4wh_1 + w(w+1)] \tag{B.7}$$

$$AC(w,h_0,h_1) = \frac{1}{(1-w)^2} [-(3+w)h_0 + 4(w+1)h_1 - (1+3w)] \tag{B.8}$$

$$AD(w,h_0,h_1) = \frac{1}{(1-w)^2} (2h_0 - 4h_1 + 2) \tag{B.9}$$

$$AB1(w,\rho_0\hat{\theta}_0,\rho_1\hat{\theta}_1) = [(w+1)(1-w^2)/2-2(1-w^3)/3]\rho_0\hat{\theta}_0 + [(1-w^3)/3-w(1-w^2)/2]\rho_1\hat{\theta}_1 \quad (B.10)$$

$$AC1(w,\rho_0\hat{\theta}_0,\rho_1\hat{\theta}_1) = [(w+1)(1-w^3)/3-2(1-w^4)/4]\rho_0\hat{\theta}_0 + [(1-w^4)/4-w(1-w^3)/3]\rho_1\hat{\theta}_1 \quad (B.11)$$

$$AD1(w,\rho_0\hat{\theta}_0,\rho_1\hat{\theta}_1) = [(w+1)(1-w^4)/4-2(1-w^5)/5]\rho_0\hat{\theta}_0 + [(1-w^5)/5-w(1-w^4)/4]\rho_1\hat{\theta}_1 \quad (B.12)$$

whence

$$LHS\left[\rho_0\hat{\theta}_0,\rho_1\hat{\theta}_1,w,h_0,h_1,\phi_0,\phi_1,\left(\frac{\phi}{Pr}\right)_0,\left(\frac{\phi}{Pr}\right)_1\right] = AB(w,h_0,h_1)\ AB2(w,\rho_0\hat{\theta}_0,\rho_1\hat{\theta}_1) + AC(w,h_0,h_1) \times AC2(w,\rho_0\hat{\theta}_0,\rho_1\hat{\theta}_1)+AD(w,h_0,h_1)AD2(w,\rho_0\hat{\theta}_0,\rho_1\hat{\theta}_1) \quad (B.13)$$

and

$$AH(w,\rho_0\hat{\theta}_0,\rho_1\hat{\theta}_1) = -\frac{1}{(1-w)^2}[-4wAB1(w,\rho_0\hat{\theta}_0,\rho_1\hat{\theta}_1) + 4(w+1)\ AC1(w,\rho_0\hat{\theta}_0,\rho_1\hat{\theta}_1)-4AD1(w,\rho_0\hat{\theta}_0,\rho_1\hat{\theta}_1)] \quad (B.14)$$

And the variables AB2, AC2, and AD2 in equations (B.13) and (B.14) are defined by the following functionals:

$$AB2(w,\rho_0\hat{\theta}_0,\rho_1\hat{\theta}_1) = [(w+1)(1-w^2)/2-2(1-w^3)/3]\frac{\partial}{\partial\xi}(\rho_0\hat{\theta}_0) +[(1-w^3)/3-w(1-w^2)/2]\frac{\partial}{\partial\xi}(\rho_1\hat{\theta}_1) \quad (B.15)$$

$$AC2(w,\rho_0\hat{\theta}_0,\rho_1\hat{\theta}_1) = [(w+1)(1-w^3)/3-2(1-w^4)/4]\frac{\partial}{\partial\xi}(\rho_0\hat{\theta}_0) +\left[(1-w^4)/4-w(1-w^3)/3\right]\frac{\partial}{\partial\xi}(\rho_1\hat{\theta}_1) \quad (B.16)$$

$$AD2(w,\rho_0\hat{\theta}_0,\rho_1\hat{\theta}_1) = [(w+1)(1-w^4)/4-w(1-w^5)/5]\frac{\partial}{\partial\xi}(\rho_0\hat{\theta}_0)$$

$$+[(1-w^5)/5-w(1-w^4)/4]\frac{\partial}{\partial\xi}(\rho_1\hat{\theta}_1) \qquad (B.17)$$

$$RA(w,h_0,\phi_0,\rho_0\hat{\theta}_0) = h_w \frac{\phi_0}{\rho_0\hat{\theta}_0} - (1-w)\left(\frac{\partial h^*}{\partial u^{**}}\right)_{u^{**}=w} \frac{\left(\frac{\phi}{Pr}\right)_0}{\rho_0\hat{\theta}_0} \qquad (B.18)$$

where

$$h_w = AB(w,h_0,h_1)+wAC(w,h_0,h_1)+w^2AD(w,h_0,h_1) \qquad (B.19)$$

$$\left(\frac{\partial h^*}{\partial u^{**}}\right)_{u^{**}=w} = AC(w,h_0,h_1)+2wAD(w,h_0,h_1) \qquad (B.20)$$

$$RB(w,h_0,h_1,\phi_0,\phi_1,\rho_0\hat{\theta}_0,\rho_1\hat{\theta}_1)$$

$$= \frac{1}{(1-w)^2}\,[RB1(w,h_0,h_1,\phi_0,\phi_1,\rho_0\hat{\theta}_0,\rho_1\hat{\theta}_1)$$

$$+ RB2(w,h_0,h_1,\phi_0,\phi_1,\rho_0\hat{\theta}_0,\rho_1\hat{\theta}_1)] \qquad (B.21)$$

The functional relations RB1 and RB2 in the above equations are defined as follows:

$$RB1(w,h_0,h_1,\phi_0,\phi_1,\rho_0\hat{\theta}_0,\rho_1\hat{\theta}_1) = AC(w,h_0,h_1)\left\{\left[(w+1)\right.\right.$$

$$\times\ [1-w-(1-w^2)/2]-2[(1-w^2)/2-(1-w^3/3]\left(\frac{\phi_0+\left(\frac{\phi}{Pr}\right)_0}{\rho_0\hat{\theta}_0}\right)$$

$$\left.\left. + 4[(1-w^2)/2-(1-w^3)/3-w(1-w^2)/2]\left(\frac{\phi_1+\left(\frac{\phi}{Pr}\right)_1}{\rho_1\hat{\theta}_1}\right)\right\} \qquad (B.22)$$

$$RB2(w,h_0,h_1,\phi_0,\phi_1,\rho_0\hat{\theta}_0,\rho_1\hat{\theta}_1) = 2AD(w,h_0,h_1)$$

$$\times\left\{\left[(w+1)[(1-w^2)/2-(1-w^3)/3]-2[(1-w^3/3\right.\right.$$

$$\left.-(1-w^4)/4\right]\left(\frac{\phi_0+\left(\frac{\phi}{Pr}\right)_0}{\rho_0\hat{\theta}_0}\right)+4\left[(1-w^3)/3-(1-w^4)/4\right.$$

$$\left.\left.-w[(1-w^2)/2-(1-w^3)/3]\right]\left(\frac{\phi_1+\left(\frac{\phi}{Pr}\right)_1}{\rho_1\hat{\theta}_1}\right)\right\} \qquad (B.23)$$

$$RC = 0 \qquad (B.24)$$

$$RD(\hat{U}_e,h_e,w,\phi_0,\phi_1,\rho_0\hat{\theta}_0,\rho_1\hat{\theta}_1) = \frac{\hat{U}_e^2}{g_c J h_e}\left\{\left[(w+1)[1-w\right.\right.$$

$$\left.-2(1-w^2)/2+(1-w^3)/3]-2[(1-w^2)/2-2(1-w^3)/3\right.$$

$$\left.+(1-w^4)/4\right]\frac{\phi_0}{\rho_0\hat{\theta}_0}+4\left[(1-w^2)/2-2(1-w^3)/3+(1-w^4)/4\right.$$

$$\left.\left.-w[1-w-2(1-w^2)/2+(1-w^3)/3]\right]\frac{\phi_1}{\rho_1\hat{\theta}_1}\right\}\Big/(1-w)^2 \qquad (B.25)$$

whence

$$RHS\left(\rho_0\hat{\theta}_0,\rho_1\hat{\theta}_1,w,h_0,h_1,\phi_0,\phi_1,\left(\frac{\phi}{Pr}\right)_0,\left(\frac{\phi}{Pr}\right)_1\right)$$

$$=RA(w,h_0,\phi_0,\rho_0\hat{\theta}_0) + RB(w,h_0,h_1,\phi_0,\phi_1,\rho_0\hat{\theta}_0,\rho_1\hat{\theta}_1)$$

$$+RC+RD(\hat{U}_e,h_e,w,\phi_0,\phi_1,\rho_0\hat{\theta}_0,\rho_1\hat{\theta}_1) \qquad (B.26)$$

The differential equation governing the conservation of energy is obtained by combining equations (B.13, (B.14) and (B.26) to give

$$\frac{\partial h_1}{\partial \xi} = (\text{RHS} - \text{LHS})/AH \qquad (B.27)$$

The integration of (B.27) was accomplished simultaneously with the momentum equation, at which time simultaneous values for $\partial(\rho_0 \hat{\theta}_0)/\partial\xi$ and $\partial(\rho_1 \hat{\theta}_1)/\partial\xi$ are available.

APPENDIX C

METHOD FOR DERIVATION OF POLYNOMIALS FOR REAL GAS PROPERTIES

The real gas properties of nitrogen tabulated by Ahtye in reference 14 form the basis for the real gas properties used in this study. This source appears satisfactory primarily because it provided adequate information for a least squares curve fit of the desired property variables in terms of enthalpy.

The coefficients in the property polynomials used in this study were taken from reference 15. The method of their derivation is presented here for completeness only. The tabulated data of reference 14 were fitted in generally overlapping segments with seventh degree polynomials in the enthalpy ratio, expressed in the following form:

$$\psi = \sum_{i=0}^{7} a_i \left(\frac{h}{h_r}\right)^i \qquad (C.1)$$

where

$$\psi \equiv \begin{cases} \dfrac{\rho}{\rho_r} \\ \dfrac{\rho\mu}{\rho_r\mu_r} \\ \dfrac{\rho\mu}{\rho_r\mu_r Pr} \end{cases} \qquad (C.2)$$

and the variables designated ρ_r, μ_r, h_r are respectively the reference density, dynamic viscosity and enthalpy. These reference properties are chosen to normalize the related variables, and hence reduce the overall magnitude of the coefficients, a_i.

The a_i, (i = 0, 1, 2, . . 7) are obtained by solving the simultaneous systems of equations formed by writing the equation (C.1) for at least eight values of h/h_r in the segment of property variation that is being curve fitted. Thus the equations obtained for any of the properties in equivalence equation (C.2) can be written in the following form:

$$\begin{bmatrix} 1 & (h/h_r)_0 & (h/h_r)_1^2 & \ldots (h/h_r)_0^7 \\ 1 & (h/h_r)_1 & (h/h_r)_1^2 & \ldots (h/h_r)_1^7 \\ \cdot & & \cdots & \\ \cdot & & \cdots & \\ \cdot & & \cdots & \\ 1 & (h/h_r)_7 & (h/h_r)_7^2 & \ldots (h/h_r)_7^7 \\ \cdot & & \cdots & \\ \cdot & & \cdots & \\ 1 & (h/h_r)_{7+j}^2 & (h/h_r)_{7+j}^2 & \ldots (h/h_r)_{7+j}^7 \end{bmatrix} \begin{bmatrix} a_0 \\ a_1 \\ a_2 \\ a_3 \\ a_4 \\ a_5 \\ a_6 \\ a_7 \end{bmatrix} = \begin{bmatrix} \psi_0 \\ \psi_1 \\ \psi_2 \\ \psi_3 \\ \psi_4 \\ \psi_5 \\ \psi_6 \\ \psi_7 \\ \psi_{7+j} \end{bmatrix} \qquad (C.3)$$

In the above equation, $(h/h_r)_i$ is the enthalpy ratio taken at the i-th location, and ψ_i is the value of the dependent variable whose seventh degree polynomial in terms of h/h_r is being sought. The form of equation (C.3) is general, and the development in this appendix applies to the other properties stated in equation (C.2). If j=0 the system (C.3) is compatible and can be solved for the a_i's exactly by well-known method of Gaussian elimination. When j>0, then the system has a redundancy of j, and a solution may be sought in which some criterion of error minimization is satisfied. In reference 15, the criterion guaranteed a least square deviation at the curve fit points.

The reference values of ρ_r, μ_r, h_r are presented in Table C-1, and the coefficients in the seventh degree polynomials for nitrogen gas properties are given in Table C-2 for pressure in the range 0.001 to 100 atmospheres. The values of specific heat at constant pressure are given in Table C-3 as a function of h/h_r for the same pressure range.

Table C-1

REFERENCE NITROGEN PROPERTIES

h_r= 0.2160E 09 [ft^2/sec^2]

Pressure Atm.	ρ_r $\frac{Slug}{ft^3}$	$\rho_r \mu_r$ $\frac{Slug}{ft^4\ Sec.}$
.0001	0.10398E-07	0.21380E-13
.001	0.96395E-07	0.20898E-12
.01	0.88964E-06	0.20472E-11
.1	0.81765E-05	0.20028E-10
1	0.74780E-04	0.19501E-09
10	0.68241E-03	0.18991E-08
100	0.62148E-02	0.18432E-07

Table C-2

Coefficients for Nitrogen Property Polynomials

$$\phi = \rho\mu/\rho_r\mu_r$$

Pressure Atm.	Enthalpy Ratio Range	a_0	a_1	a_2	a_3	a_4	a_5	a_6	a_7
.0001	$.01 < h/h_r \leq .35$	0.48989169E 01	-0.84212749E 02	0.11310220E 04	-0.87493920E 04	0.37942339E 05	-0.88073029E 05	0.95424590E 05	-0.30673710E 05
	$.35 < h/h_r \leq 2.0674$	0.17681660E 01	-0.16778930E 01	0.14490189E 01	-0.30141160E 00	-0.67942970E 00	0.62419470E 00	-0.20878629E 00	0.24949069E-01
.001	$.01 < h/h_r \leq .2$	0.50392869E 01	-0.89063559E 02	0.12871770E 04	-0.11846630E 05	0.74102578E 05	-0.32766459E 06	0.91924249E 06	-0.11640479E 07
	$.2 < h/h_r \leq 2.091$	0.16891240E 01	-0.94594999E 00	-0.83889100E 00	0.30425700E 01	-0.32358139E 01	0.16674720E 01	-0.41939690E 00	0.40754569E-01
.01	$.01 < h/h_r \leq .2907$	0.50885029E 01	-0.83690089E 02	0.10240439E 04	-0.66701059E 04	0.20333999E 05	-0.13154349E 05	-0.61699999E 05	0.98628698E 05
	$.2907 < h/h_r \leq 2.0766$	0.19957309E 01	-0.30782390E 01	0.47468689E 01	-0.40815699E 01	0.14429980E 01	0.19863240E 00	-0.27641150E 00	0.53207940E-01
.10	$.01 < h/h_r \leq .3326$	0.51900749E 01	-0.84870889E 02	0.10530110E 04	-0.73942129E 04	0.28891370E 05	-0.60685789E 05	0.60907089E 05	-0.20057339E 05
	$.3326 < h/h_r \leq 2.0$	0.19063280E 01	-0.23219009E 01	0.24773660E 01	-0.88921810E 00	-0.84278230E 00	0.99904820E 00	-0.38065640E 00	0.51407450E-01
1.0	$.00508 < h/h_r \leq .2946$	0.53791619E 01	-0.90071339E 02	0.11118380E 04	-0.71636940E 04	0.20280690E 05	-0.15067710E 04	-0.10507099E 06	0.14810470E 06
	$.2946 < h/h_r \leq 2.0418$	0.20023789E 01	-0.26414099E 01	0.24662789E 01	-0.85702179E 00	-0.28501190E 01	0.24115890E 01	-0.85734890E 00	0.11433510E 00
10.0	$.01 < h/h_r \leq .28984$	0.54935669E 01	-0.91457780E 02	0.11491869E 04	-0.78532869E 04	0.26444740E 05	-0.28648350E 05	-0.48467059E 05	0.10399339E 06
	$.28984 < h/h_r \leq 2.0014$	0.24336319E 01	-0.55602919E 01	0.10441110E 02	-0.11061969E 02	0.63884189E 01	-0.18064220E 01	0.14837389E 00	0.17995410E-01
100.0	$.01 < h/h_r \leq .2785$	0.61077189E 01	-0.14522409E 03	0.29901110E 04	-0.36598659E 05	0.25713459E 06	-0.10154590E 07	0.20901579E 07	-0.17416719E 07
	$.2785 < h/h_r \leq 2.0$	0.22902369E 01	-0.36396299E 01	0.32955679E 01	0.63547710E 00	-0.32922269E 01	0.22973579E 01	-0.64834770E 00	0.63883030E-01

Table C-2
(continued)

$$\phi/Pr = \rho\mu/\rho_r\mu_r Pr$$

Pressure Atm.	Enthalpy Ratio Range	a_0	a_1	a_2	a_3	a_4	a_5	a_6	a_7
.0001	$.01518 < \frac{h}{h_r} \leq .3$	0.687096096E 01	-0.14532950E 03	0.29202420E 04	-0.40501419E 05	0.34477869E 06	-0.16727230E 07	0.42110190E 07	-0.42423630E 07
	$.30 < \frac{h}{h_r} \leq 2.0764$	0.39254709E 01	-0.63758949E 01	0.75305539E 01	-0.34988269E 01	-0.31510919E 01	0.46257729E 01	-0.20249110E 01	0.30837750E 00
.001	$.01 < \frac{h}{h_r} \leq .2181$	0.67920819E 01	-0.11193600E 03	0.12521560E 04	-0.63096739E 04	0.87071529E 03	0.11809940E 06	-0.41758680E 06	0.44612779E 06
	$.2181 < \frac{h}{h_r} \leq .5$	0.81321719E 00	0.98299509E 01	-0.14939629E 02	0.13736139E 01	0.	0.	0.	0.
	$.5 < \frac{h}{h_r} \leq 2.091$	0.39484770E 01	-0.53553149E 01	0.42249269E 01	-0.10334159E 01	-0.11736690E 01	0.10101730E 01	-0.27862529E 00	0.24950340E-01
.01	$.01 < \frac{h}{h_r} \leq .3$	0.69986759E 01	-0.12159050E 03	0.15538029E 04	-0.11196669E 05	0.43611009E 05	-0.84796229E 05	0.68628389E 05	-0.13159460E 05
	$.3 < \frac{h}{h_r} \leq 2.0766$	0.22901999E 01	0.29276770E 01	-0.11688709E 02	0.13504729E 02	-0.69089879E 01	0.96525469E 00	0.40813620E 00	-0.11814439E 00
.10	$.01 < \frac{h}{h_r} \leq .35$	0.70070889E 01	-0.10894790E 03	0.11037330E 04	-0.46936449E 04	-0.32553089E 04	0.94300729E 05	-0.28307600E 06	0.26959439E 06
	$.35 < \frac{h}{h_r} \leq 2.0$	0.29033969E 01	-0.13356730E 01	-0.10176670E 01	0.16860010E 01	-0.15360329E 01	0.10567489E 01	-0.40494930E 00	0.60863939E-01
1.0	$.00508 < \frac{h}{h_r} \leq .4$	0.69456239E 01	-0.10128180E 03	0.10706180E 04	-0.64511379E 04	0.21416850E 05	-0.36124440E 05	0.24658450E 05	-0.11855330E 04
	$.4 < \frac{h}{h_r} \leq 2.0418$	-0.70408939E 01	0.63920749E 02	-0.16899220E 03	0.22239780E 03	-0.16106790E 03	0.63913349E 02	-0.12590539E 02	0.89416499E 00
10.0	$.01 < \frac{h}{h_r} \leq .45$	0.76473840E 01	-0.13631880E 03	0.17044809E 04	-0.11501510E 05	0.41581109E 05	-0.77864250E 05	0.66311499E 05	-0.16067690E 05
	$.45 < \frac{h}{h_r} \leq 2.0014$	0.25206509E 01	-0.25365390E 00	-0.47839460E 00	-0.22938199E 01	0.33677480E 01	-0.16458739E 01	0.28332780E 00	-0.20691629E-02
100.0	$.01451 < \frac{h}{h_r} \leq .4571$	0.79054969E 01	-0.12150680E 03	0.11164659E 04	-0.42796180E 04	0.22261470E 03	0.43827789E 05	-0.11241270E 06	0.87857608E 05
	$0.4571 < \frac{h}{h_r} \leq 2.2865$	0.15796050E 01	0.37804409E 01	-0.74781239E 01	0.36810679E 01	0.16344839E 01	-0.24808899E 01	0.97487289E 00	-0.13239790E 00

Table C-2
(concluded)

Density Ratio ρ_r/ρ

Pressure Atm.	Enthalpy Ratio Range	a_0	a_1	a_2	a_3	a_4	a_5	a_6	a_7
.0001	$.01 < \frac{h}{h_r} \leq .4$	-0.74309900E-02	0.40124589E 01	-0.35437389E 02	0.46337879E 03	-0.31935100E 04	0.11423440E 05	-0.20550279E 05	0.14680789E 05
	$.39971 < \frac{h}{h_r} \leq 2.0674$	0.45696390E 00	0.69044140E 00	-0.40385420E 00	0.32477169E 00	-0.10000540E-02	-0.90701629E-01	0.20436659E-01	0.33214290E-02
.001	$.01 < \frac{h}{h_r} \leq .4$	-0.70452759E-02	0.34589639E 01	-0.15662820E 02	0.83613370E 02	0.47418039E 02	-0.20357600E 04	0.62572470E 04	-0.58172330E 04
	$.4 < \frac{h}{h_r} \leq 2.091$	0.26045030E 00	0.17098119E 01	-0.22763070E 01	0.16119710E 01	0.14857499E 00	-0.76251020E 00	0.35536480E 00	-0.51280219E-01
.01	$.00516 < \frac{h}{h_r} \leq .3571$	-0.29208580E-02	0.29761539E 01	-0.12036160E 02	0.10341100E 03	-0.56260049E 03	0.19085220E 04	-0.39144180E 04	0.34866799E 04
	$.3571 < \frac{h}{h_r} \leq 2.0766$	0.24460179E 00	0.14109360E 01	-0.47511289E 00	-0.25292119E 01	0.50412910E 01	-0.39013039E 01	0.13942699E 01	-0.19028900E 00
.10	$.00515 < \frac{h}{h_r} \leq .3411$	-0.50878490E-03	0.24666060E 01	-0.25256269E 01	-0.13251179E 02	0.11657599E 03	-0.15882719E 01	-0.14930210E 04	0.25308680E 04
	$.3411 < \frac{h}{h_r} \leq 2.0$	0.18135360E 00	0.17127939E 01	-0.16510770E 01	0.32155120E 00	0.13739029E 01	-0.14138970E 01	0.55189880E 00	-0.78224880E-01
1.0	$.00508 < \frac{h}{h_r} \leq .4$	-0.10665800E-02	0.23295859E 01	-0.46026419E 01	0.15823960E 02	-0.35376849E 02	0.18929320E 03	-0.76800639E 03	0.93670900E 03
	$.4 < \frac{h}{h_r} \leq 2.0418$	-0.14435600E 00	0.37273020E 01	-0.68165659E 01	0.71131829E 01	-0.34185129E 01	0.32422929E 00	0.28761370E 00	-0.73482079E-01
10.0	$.00676 < \frac{h}{h_r} \leq .355$	-0.91251619E-03	0.21088570E 01	-0.35819809E 01	0.57680069E 01	0.30426349E 02	-0.94154590E 02	-0.66973879E 02	0.26063950E 03
	$.355 < \frac{h}{h_r} \leq 2.0014$	0.41342609E-01	0.20807429E 01	-0.21952619E 01	0.11918870E 01	0.25558309E 00	-0.58808230E 00	0.24894100E 00	-0.35414969E-01
100.0	$.00783 < \frac{h}{h_r} \leq .3526$	0.82283460E-03	0.18284919E 01	-0.17727660E 01	-0.36755460E 01	0.43142670E 02	-0.57897759E 02	-0.15374839E 03	0.29318060E 03
	$.3526 < \frac{h}{h_r} \leq 2.0$	-0.51321019E-01	0.22681859E 01	-0.22C81339E 01	0.89989850E 00	0.56967939E 00	-0.69500180E 00	0.24538630E 00	-0.29580630E-01

Table C-3

Nitrogen Specific Heat At Constant Pressure

h/h_r	Pressure Atmospheres						
	.0001	.001	.01	.1	1	10	100
0.02	0.24936	0.24936	0.24936	0.24936	0.24936	0.24936	0.24936
0.04	0.26205	0.26205	0.26205	0.26205	0.26205	0.26205	0.26205
0.06	0.28279	0.28279	0.28279	0.28279	0.28279	0.28279	0.28279
0.08	0.29419	0.29419	0.29419	0.29419	0.29419	0.29419	0.29419
0.10	0.30154	0.30154	0.30154	0.30154	0.30154	0.30154	0.30154
0.12	0.30547	0.30540	0.30533	0.30533	0.30533	0.30533	0.30533
0.14	0.30679	0.30806	0.30807	0.30824	0.30830	0.30836	0.30836
0.16	0.32186	0.31459	0.31166	0.31106	0.31086	0.31066	0.31066
0.18	0.34731	0.32451	0.31608	0.31368	0.31288	0.31214	0.31213
0.20	0.46052	0.34945	0.32481	0.31671	0.31476	0.31393	0.31329
0.22	0.64175	0.47521	0.38200	0.33628	0.32125	0.31677	0.31479
0.24	0.89369	0.69650	0.47562	0.37534	0.33518	0.32144	0.31694
0.26	1.21545	0.89846	0.59708	0.44487	0.36511	0.33175	0.32097
0.28	1.56753	1.08842	0.78043	0.54814	0.41121	0.35065	0.32770
0.30	1.86564	1.29666	0.98235	0.66389	0.48412	0.38070	0.33895
0.32	2.15032	1.53052	1.16536	0.80801	0.56958	0.42296	0.35586
0.34	2.42155	1.78088	1.34263	0.96881	0.66646	0.48163	0.38085
0.36	2.67935	2.04188	1.53074	1.11990	0.78284	0.54722	0.41259
0.38	2.92841	2.28255	1.72244	1.27001	0.89864	0.62229	0.45211
0.40	3.16850	2.52218	1.91771	1.42378	1.01599	0.70521	0.49748
0.42	3.39776	2.76079	2.11539	1.57936	1.13625	0.78962	0.55035
0.44	3.61619	2.99838	2.30613	1.73933	1.25908	0.87753	0.60599
0.46	3.82379	3.23532	2.49584	1.89274	1.38511	0.97033	0.66568
0.48	4.02055	3.43523	2.68451	2.04446	1.50645	1.06157	0.72832
0.50	4.13995	3.62256	2.88770	2.19447	1.62641	1.15317	0.78993
0.52	4.33892	3.79731	3.05278	2.34925	1.74618	1.24378	0.85153
0.54	4.53587	3.95949	3.20698	2.48436	1.85837	1.33372	0.91314
0.56	4.73081	4.10910	3.35028	2.51182	1.96637	1.42301	0.97475
0.58	5.44268	4.21829	3.48269	2.73162	2.06852	1.51227	1.03635
0.60	5.80213	4.35225	3.59006	2.83669	2.16945	1.60184	1.09796
0.62	6.06475	4.47770	3.70399	2.94373	2.26723	1.69141	1.15957
0.64	6.23057	4.59462	3.80957	3.04524	2.36186	1.78098	1.22117
0.66	6.29956	4.70303	3.90680	3.14122	2.46330	1.87054	1.28278
0.68	6.27174	4.97552	3.99568	3.23167	2.54490	1.96011	1.34438
0.70	6.14710	5.07758	4.07621	3.35117	2.61794	2.04958	1.40599
0.72	5.92564	5.14248	4.23461	3.42082	2.68242	2.13925	1.46760
0.74	5.60736	5.17023	4.28417	3.47444	2.73834	2.22882	1.52920
0.76	5.03647	5.16082	4.30712	3.51203	2.78571	2.31838	1.59081
0.78	4.69029	5.11426	4.30348	3.53358	2.82575	2.40795	1.65242
0.80	4.36782	5.03053	4.27323	3.55145	2.88059	2.49752	1.71402
0.82	4.06905	4.91478	4.23390	3.53902	2.93544	2.58709	1.77563
0.84	3.79400	4.75691	4.15148	3.50727	2.99028	2.67656	1.83723
0.86	3.54266	4.56084	4.03810	3.45620	3.04512	2.76622	1.89884
0.88	3.31503	4.32657	3.89376	3.40948	3.09996	2.85579	1.96045
0.90	3.11111	4.06258	3.71846	3.32430	3.15480	2.94536	2.02205
0.92	2.93090	3.79526	3.54599	3.20861	3.20965	3.03493	2.08366
0.94	2.77440	3.46325	3.31484	3.06243	3.26449	3.12449	2.14527
0.96	2.64162	3.06655	3.03632	2.88574	3.31933	3.21406	2.20687
0.98	2.50924	2.60514	2.71043	2.67855	3.37417	3.30363	2.26848
1.00	2.34521	2.00206	2.28159	2.44086	3.42902	3.39320	2.33008
1.02	2.19107	1.42480	1.87247	2.19979	3.48386	3.48277	2.39169
1.04	2.04681	0.97522	1.49363	1.98205	3.53870	3.57233	2.45330
1.06	1.91244	0.62815	1.13989	1.76431	3.59354	3.66190	2.51490
1.08	1.78795	0.37551	0.80321	1.54657	3.64838	3.75147	2.57651
1.10	1.67335	0.35025	0.48017	1.32883	3.70323	3.84104	2.63811

APPENDIX D

EVALUATION OF ESSENTIAL BOUNDARY-LAYER PARAMETERS

The expression for the characteristic boundary-layer parameters will be derived in terms of the free parameters $\rho_i\hat{\theta}_i$ and h_i, i=0,1 that were used in Appendix A in the determination of the coefficients of the approximating functions, and the shock intensity parameter, w.

The skin friction coefficient, C_f, in the shock-fixed reference can be written as follows:

$$\hat{C}_f = \frac{\mu_w \left(\frac{\partial \hat{u}}{\partial \hat{y}}\right)_w}{\rho_e \hat{U}_e^2}$$

whence

$$\hat{C}_f \sqrt{\hat{Re}_L} = \frac{\phi_0}{\rho_0 \hat{\theta}_0}$$

where

$$\phi_0 = \left.\frac{\rho\mu}{\rho_e \mu_e}\right]_{u^{**}=w}$$

and

$$\theta_0 = \left(\frac{\partial u^{**}}{\partial \hat{\eta}}\right)^{-1}_{u^{**}=w} \qquad \text{(D.1)}$$

To facilitate the comparison of equation (D.1) with exact solutions obtained by Mirels in the shock-fixed reference, the corresponding equation for skin friction coefficient developed from reference 1 can be written in following form

$$\hat{C}_f \sqrt{\hat{Re}_L} = \sqrt{2\hat{\xi}}/f''(0) \qquad (D.2)$$

where f is a function of the similarity variable η_m given in equation (4.10), and $f''(0)$, evaluated at $\eta_m=0$, is independent of $\hat{\xi}$ in the entire range $0 \leq \hat{\xi} \leq 1$.

In a coordinate system which is stationary with respect to the wall, the value of the skin friction coefficient can be obtained in a form similar to equation (D.1). This is as follows:

$$C_f \sqrt{Re_L} = \frac{\phi_0}{\rho_0 \theta_0} \qquad (D.3a)$$

where

$$\phi_0 = \left(\frac{\rho \mu}{\rho_e \mu_e} \right)_{u^*=0}$$

$$\theta_0 = \left(\frac{\partial u^*}{\partial \eta} \right)^{-1}_{u^*=0} \qquad (D.3b)$$

On account of the difference in the stretching of the transverse coordinate, and the difference between the nondimensional velocities in the shock-fixed and the fixed-wall references, the inverse of the gradient of the nondimensional velocities in the two references are not equal. For the same

reasons, the skin friction coefficients given by equations (D.1) and (D.3) cannot have the same values, but are related through some multiplying factor. Equation (D.3) determines the skin friction coefficient in the physical coordinate system. In order to relate equation (D.3) to (D.1), it is facile to use the fundamental transformation equations (2.7a), (2.7h) and (5.11b), the essential parts of which are reproduced here:

$$\eta = \sqrt{\frac{U_e L}{\nu_e}} \frac{y}{L} \qquad (2.7h)$$

$$\hat{\eta} = \sqrt{\frac{\hat{U}_e L}{\nu_e}} \frac{y}{L} \qquad (5.11b)$$

$$u^* = \frac{u}{U_e} \qquad (2.7a)$$

$$u^* = \frac{w - u^{**}}{w-1} \qquad (D.4)$$

and using the definition of the inverse of the gradient of the nondimentional velocity gradient:

$$\theta = \left(\frac{\partial u^*}{\partial \eta}\right)^{-1}$$

$$\hat{\theta} = \left(\frac{\partial u^{**}}{\partial \hat{\eta}}\right)^{-1} \qquad (D.5)$$

Then the relationship between θ and $\hat{\theta}$ can be obtained in the form

$$\frac{1}{\theta} = - \frac{1}{(w-1)^{3/2}} \frac{1}{\hat{\theta}} \qquad (D.6)$$

and from which the skin friction coefficients given by equations (D.1) and (D.3) are related by

$$C_f\sqrt{Re_L} = -\frac{1}{(w-1)^{3/2}}\ \hat{C}_f\sqrt{\hat{Re}_L} \tag{D.7}$$

The heat transfer at the wall is estimated from the heat conduction at the wall surface or from convective exchange between the wall and the freestream:

$$q = -\frac{\mu}{Pr}\left(\frac{\partial h}{\partial y}\right) = \frac{\mu h_e}{Pr}\frac{\sqrt{Re}}{L}\left(\frac{\partial h^*}{\partial \hat{\eta}}\right) \tag{D.8}$$

$$q = G(h_e - h_w) \tag{D.9}$$

where G is the unit heat convective coefficient of the wall surface. Combining equation (D.8) and (D.9) yields the non-dimensional Nusselt number, Nu, given by the following relation:

$$Nu(1-h_0) = \frac{1}{\hat{\theta}_0}\left(\frac{\partial h^*}{\partial u^{**}}\right)_{u^{**}=w}\sqrt{\hat{Re}_L} \tag{D.10}$$

In addition to the skin friction and convective coefficient defined above, the following boundary-layer parameters are defined below:

i. Boundary-Layer Thickness

$$\delta = \frac{L}{\sqrt{Re_L}}\int_0^{U_e^*}\theta\ du^* \tag{D.11}$$

ii. Boundary-Layer Displacement Thickness

$$\delta^* = \frac{L}{\sqrt{Re_L}} \int_0^{U_e^*} (\theta - u^* \rho^* \theta) du^* \qquad (D.12)$$

iii. Boundary-Layer Momentum Thickness

$$\delta^{**} = \frac{L}{\sqrt{Re_L}} \int_0^{U_e^*} \rho^* \theta (u^* - u^{*2}) du^* \qquad (D.13a)$$

iv. Boundary-Layer Energy Dissipation Thickness

$$\delta^{***} = \frac{L}{\sqrt{Re_L}} \int_0^{U_e^*} \rho^* \theta u^* (1 - u^{*2}) du^* \qquad (D.13b)$$

In the above integral equations, it is assumed the outer edge of the boundary layer is adequately located at the point where $U_e^* = 0.995$. This choice is consistent with standard practice in boundary-layer analysis, since in all of these equations, it can be observed that the upper limits of integration cannot be unity. At $u^*=1$, the integrals are unbounded.

There is some arbitrariness in literature in the definition of the Reynolds number associated with the study of shock induced flows over a flat plate. In a recent work, Ackroyd (reference 2) formulated a Reynolds number based on the relative motion between the freestream and moving flat surface. In this case Reynolds number was given by

$$Re = \frac{\rho_e (w-1)^2 \hat{x} \hat{U}_e}{\mu_e} \qquad (D.14)$$

and for the same reasons as those stated by Ackroyd above, in reference 1, Mirels chose the following formulation

$$Re = \frac{\rho_w (w-1)^2 U_e^2 t}{\mu_w} \qquad (D.15)$$

Because Reynolds number occurs freely in all the above expressions for boundary-layer parameters, it behaves as a stretching factor. Thus the expressions in (D.14) and (D.15) do not contribute to better correlation of results, and it is the opinion of this study that they do in fact becloud the problem of comparing the results of different authors. In this study, the Reynolds number as it appears in the boundary-layer parameters above is given by the following equation:

$$Re_L = \frac{\rho_e U_e L}{\mu_e} \qquad (D.16)$$